Exploring the Conversion of Macrocyclic 2,2'-Biaryl Bis(thioureas) into Cyclic Monothioureas: An Experimental and Computational Investigation

Mateo Alajarin,[†] Carmen Lopez-Leonardo,[†] Raul-A. Orenes, [‡] Aurelia Pastor,*[†] Pilar Sanchez-Andrada,*[†] and Angel Vidal[†]

[†] Department of Organic Chemistry, Faculty of Chemistry. University of Murcia. Regional Campus of International Excellence "Campus Mare Nostrum", 30100 Murcia, Spain. E-mail: aureliap@um.es, andrada@um.es

[‡] SAI, University of Murcia. Campus de Espinardo, 30100 Murcia, Spain

ORCID ID's: Prof. M. Alajarin 000-0002-7112-5578, Dr. C. Lopez Leonardo 000-0001-8737-4280, Dr. A. Pastor 000-0003-0437-2605, Dr. P. Sánchez Andrada 000-0002-9944-8563, Dr. A. Vidal 000-0002-4347-6215.

Abstract

Macrocyclic bis(thioureas) derived from 2,2'-biphenyl and binaphthyl skeletons have been synthesized by reaction of 2,2'-diaminobiaryl and 2,2'-bis(isothiocyanato)biaryl derivatives. The splitting of these bis(thioureas) into two units of the respective cyclic monothioureas has been monitored by NMR, shedding some light on the factors that control these processes. Additionally, a computational study revealed up to three mechanistic paths for the conversion of the 2,2'-biphenyl-derived bis(thiourea) into the corresponding monothiourea. The proposed mechanisms account for the participation of a molecule of water as an efficient proton-switch, as well as for different classes of putative intermediates. The computational study also supports the ability of the thiourea group to participate in a plethora of processes, such as prototropic equilibria, sigmatropic shifts, heteroene and retro-heteroene reactions, and *cis* ⇆ *trans* isomerizations.

Introduction

In recent years, thioureas and its derivatives have been the focus of attention because of their interesting applications. Certain thiourea molecules have antiviral, antibacterial or antifungal activity.[1-6] Furthermore, the relatively high acidity of the NH thiourea protons is correlated with their strong hydrogen-bonding donor capability, a quality that has been exploited in the design of neutral receptors for anions.[7] Perhaps the most important role of thioureas in modern organic chemistry is the participation of chiral derivatives as enantioselective catalysts in a wide variety of organocatalyzed asymmetric synthesis.[8-10] Of particular relevance are examples of this kind of reactions in which chiral bis(thioureas) have been unveiled as efficient organocatalysts.[11-14] Although the conformational and hydrogen-bonding preferences of thioureas might be predictable to some extent,[15-17] additional studies seems to be still desirable, especially in the case of their cyclic varieties, which have been scarcely studied.[18]

The structural operation of linking two 2,2'-biphenylene units by means of two identical fragments has been shown to build interesting symmetrical macrocycles displaying crossed geometries.[19-22] In some cases (*e. g.* with two carbon triple bonds as linkers)[23-25] the short distance between these two fragments allows transannular reactions to occur. In the context of a wide study on the cyclization of bis(carbodiimides), we described some years ago in this same journal[26] the synthesis of the macrocyclic bis(thiourea) **1**, endowed with a 14-membered central ring and flanked by two 2,2'-biphenylene fragments (Figure 1). Interestingly, further studies demonstrated that bis(thiourea) **1** was a selective receptor for the nitrate anion.[27]

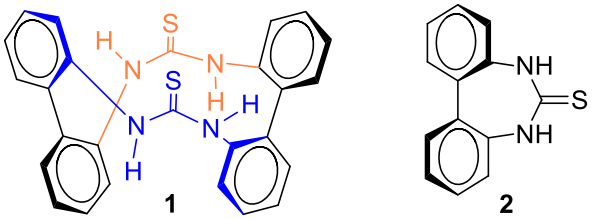

Figure 1 Structures of the bis(thiourea) **1** and the monothiourea **2**.

Recently we revisited the synthesis and properties of **1** discovering that its stability in solution was temperature- and solvent-dependent, leading either to the reversion to the starting materials, bis(amine) **3** and bis(isothiocyanate) **4**, or, rather unexpectedly, to its splitting into two molecules of the cyclic monothiourea **2**. Herein we report on these new findings by analyzing the key factors that govern the corresponding chemical equilibria involved in those transformations. Our investigations also include computational studies aimed to uncover reasonable mechanistic paths for the conversion of **1** into **2**. Notably, the chemical behavior of thioureido functions seems to be virtually unexplored by means of computational calculations and not widely tested by experiments, in contrast to the wealth of the similar information available for ureas,[28-32] especially that concerning its decomposition and hydrolysis. We believe that our results could serve to call the attention of other researchers to the potential lability of the thioureido function, especially when incorporated into more or less strained structures. In this sense, and for the sake of comparison, we have additionally included a macrocyclic 2,2'-binaphthyl bis(thiourea) and the corresponding cyclic monothiourea, analogous of **1** and **2**, in our experimental study. Their lesser degree of conformational mobility around their biaryl axis should reasonably result into more strained, and thus, more reactive cyclic structures.

Results and Discusion

Synthesis of the Macrocyclic Bis(thioureas) 1 and 8

In contrast to our previous report,[26] the macrocyclic bis(thiourea) **1** is isolated in a modest 65% yield following the reaction between 2,2'-diaminobiphenyl (**3**) and 2,2'-bis(isothiocyanato)biphenyl (**4**) in DMF at room temperature. However, when the final solution resulting from the previous reaction is heated under reflux for 2 h, the cyclic monothiourea **2** is obtained as the only product in good yield (Scheme 1).

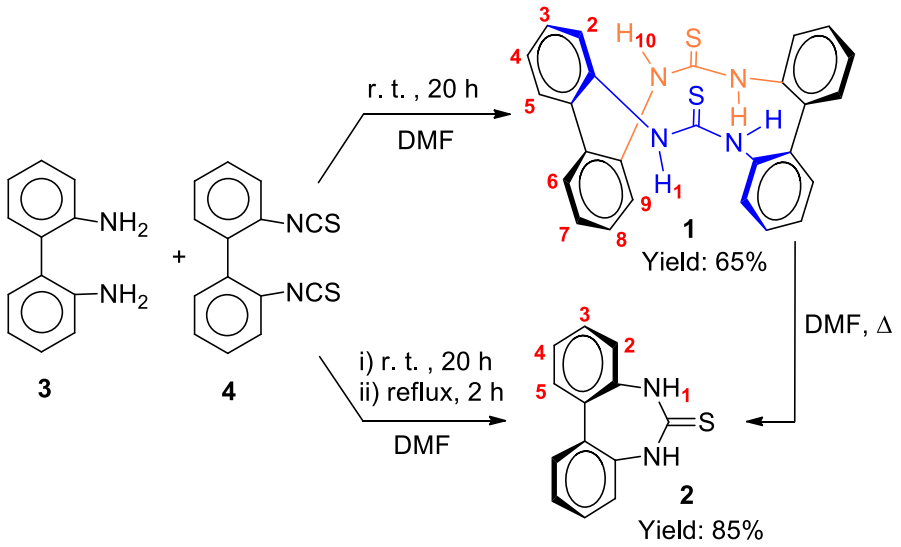

Scheme 1 Optimized reaction conditions for the synthesis of the bis(thiourea) **1** and the monothiourea **2** from 2,2'-diaminobiphenyl (**3**) and 2,2'-bis(isothiocyanato)biphenyl (**4**).

Consistently with these results, a gentle heating of a DMF-solution of **1** leads to its fast conversion into **2**. Alternatively, the cyclic thiourea **2** was independently prepared from **3** and carbon disulfide by a slight modification of the method reported by Le Fèvre.[33]

The analogous binaphthyl monothiourea **6** was obtained from 2,2'-diaminobinaphthyl (**5**) and carbon disulfide in a yield of 90%. The reaction was conducted in ethanol at 100 ºC in a sealed tube (Scheme 2). This synthetic method showed to be more efficient than the previously described one (22%).[34]

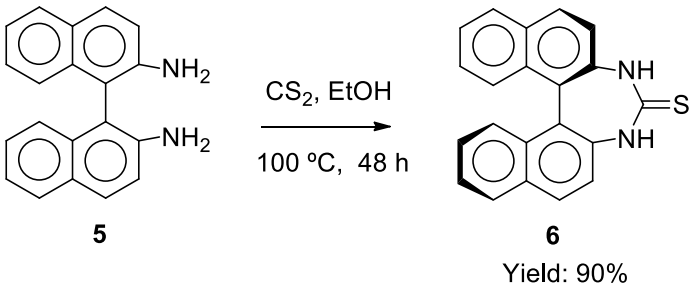

Scheme 2 Synthesis of the monothiourea **6** from 2,2'-diaminobinaphthyl (**5**) and carbon disulfide.

The macrobicyclic bis(thiourea) **8** was synthesized by stirring 2,2'-diaminobinaphthyl (**5**) and 2,2'-bis(isothiocyanato)binaphthyl (**7**) in DMF at room temperature (Scheme 3). After purification by chromatographic techniques, the bis(thiourea) **8** was isolated in 61% yield.

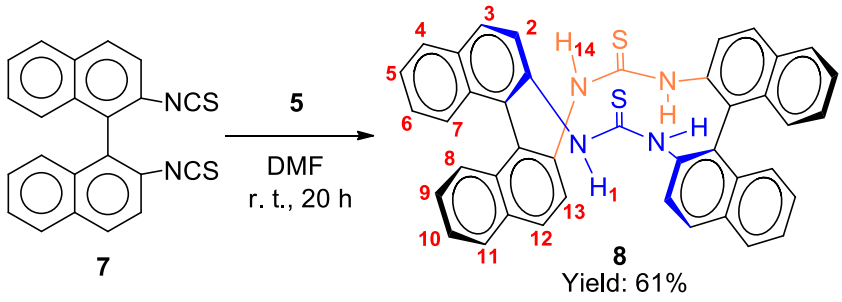

Scheme 3 Synthesis of the bis(thiourea) **8** from 2,2'-diaminobinaphthyl (**5**) and 2,2'-bis(isothiocyanato)binaphthyl (**7**).

A careful check of the ^{1}H-NMR spectra of **1** and **2** in DMF-d_7 showed that both were clearly different (Figures 2a and 2b, respectively).[35] Not surprisingly, gentle heating of the solution of the bis(thiourea) **1** turns out its spectrum identical to that of **2**. Alternatively, the NMR spectra of **1** and **2** were measured in $C_2D_2Cl_4$, a solvent with lower ability to interact by hydrogen bonding with the solute (Figures 2c and 2d). Evidently, the NMR spectra of the bis(thiourea) **1** in both, DMF-d_7 and $C_2D_2Cl_4$, display a higher complexity compared to those of the monothiourea **2**, being this intricacy more evident in $C_2D_2Cl_4$ due to a more resolved spectrum (Figure 2c).

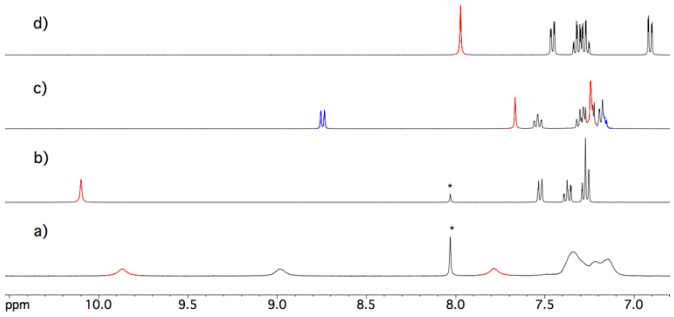

Figure 2 ^{1}H NMR spectra (400 MHz) of a) bis(thiourea) **1** in DMF-d_7, b) monothiourea **2** in DMF-d_7, c) bis(thiourea) **1** in $C_2D_2Cl_4$, and d) monothiourea **2** in $C_2D_2Cl_4$. The asterisk (*) indicates the residual signal of DMF-d_7.

Among others, the spectrum of the bis(thiourea) **1** in the less polar $C_2D_2Cl_4$, shows signals for two non-equivalent NH protons at 7.24 and 7.67 ppm (red colour). The presence of two non-equivalent NH protons is also obvious in DMF-d_7, considering that after addition of D_2O, the signals at 7.79 and 9.87 ppm (Figure 2a, red colour) disappeared. In $C_2D_2Cl_4$, resonances for two non-equivalent *ortho* disubstituted phenyl groups are also evident (Figure 2c). This pattern of signals, along with the fact that two resonances for the NH's are present, agree well with a twisted structure (*R,R* or *S,S* configuration around every biphenyl group) in which both thiourea functions adopt an *cis*, *trans* conformation (Scheme 1). The *cis*,*trans*-*R,R*/*cis*,*trans*-*S,S* spatial arrangement of **1** was confirmed by X-ray analysis (see below). In such disposition, the two biaryl subunits are equivalent on the basis of a C_2 symmetry, thus explaining the different magnetic environments for the two phenyl groups of each biaryl subunit in the ^{1}H NMR spectra. The doublet appearing at an

unusual high frequency, 8.76 ppm (Figure 2c, blue color) was assigned to the arylic *ortho* hydrogen atom H_2 (Scheme 1) located in the deshielding region of the thiocarbonyl group.

The more resolved spectrum of bis(thiourea) **1** in $C_2D_2Cl_4$ enabled us the unambiguous assignment for all protons, which was accomplished by ^{1}H,^{1}H-COSY and ^{1}H,^{1}H-NOESY experiments (Supporting Information). The NOESY/EXSY spectrum reveals not only cross-peaks due to NOE effect but also cross-peaks between mutually exchanging positions.[36,37-38] In fact, molecular modelling confirms that the concurrent *cis*,*trans* ⇆ *trans*,*cis* switch of both thiourea functions would interconvert the magnetic environments of the two phenyl groups of each biaryl fragment. The assignment of the resonances was accomplished considering the intense conformational exchange peaks between H_2/H_9 (Figure 2c in blue), H_3/H_8, H_4/H_7, H_5/H_6 and NH_1/NH_{10}.

The ^{1}H NMR spectra of **6** and **8** in DMF-d_7 and $C_2D_2Cl_4$ follow similar trends to those of **1** and **2** (Supporting Information). However, the ^{1}H NMR spectra of **8** show well-resolved signals in both solvents, indicating highly restricted intramolecular motion even in DMF. Besides, the NMR data of **8** agree well with those of the enantiomerically enriched bis(thiourea) ***R*,*R*-8** previously described by Wulff and co-workers.[39]

The HRMS data of **1-2, 6** and **8** are in accord with the proposed structures. Nevertheless, in order to investigate self-association processes in solution, their diffusion coefficients were measured in $C_2D_2Cl_4$ and DMF-d_7 (only **6** and **8**) by using PGSE techniques[40-41 42] (Table S1, Supporting Information). The *D*-values, which follow the order **2** > **6** > **1** > **8**, are consistent with the molecular sizes of the analyzed molecules. On balance, the slight discrepancies between the r_H-values of compounds **6** and **8** in $C_2D_2Cl_4$ and DMF-d_7 may be attributed to solvation effects.[43] Thus, the r_H-values point to the fact that no significant self-aggregation processes are present in the former solvent.

Diffraction quality crystals of bis(thiourea) **1** were obtained by recrystallization from $CHCl_3$/*n*-hexane (Figure 3). The X-ray analysis shows the expected C_2-symmetric crossed structures of both enantiomers, ***R*,*R*-1** and ***S*,*S*-1**. The exclusive formation of ***R*,*R*-1**/***S*,*S*-1** constitutes an interesting example of homochiral self-sorting.[44] As expected, the thiourea functionalities are arranged in a *cis*, *trans* conformation.[16, 45] The structure of **1** displays torsional angles between the two biaryl units of 109.5º, which confers to **1** a peculiar three-dimensional arrangement with a hydrophobic pocket formed by two nearly parallel aromatic rings. The lipophilicity at the proximity of two of the four NH groups may facilitate the desolvation of an incoming anionic guest.[27] The distance between the two centroids of the two nearly parallel aromatic groups is 3.90 Å. This value, beyond the optimal stacking distance of 3.5 Å, points to a weak, if any, intramolecular π-π-stacking interaction.[46] The structure of **1** shows close contacts between the sulphur atoms (S1/S1A) and the hydrogen atoms H9/H9A, placed at *ortho* position respect to the thiourea groups, *d*(C···S=C) = 3.19 Å and C-H···S angle = 128º.[47]

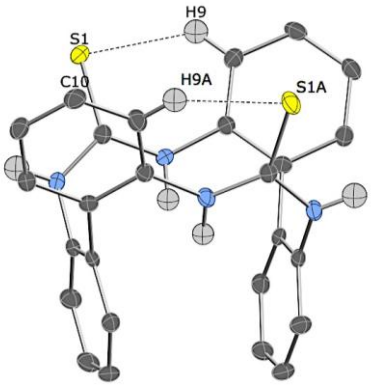

Figure 3 X-Ray structure of the bis(thiourea) **1**. ORTEP drawings with thermal ellipsoids drawn at the 50% probability level. Although only ***R*,*R*-1** is shown**,** the two enantiomers are present in the crystal lattice (Supporting Information). Some aromatic protons have been omitted for clarity.

Crystals of the monothiourea **2** suitable for X-ray analysis were obtained by recrystallization from acetonitrile (Figure 4). As presumed, the thiourea group in **2** is in an *cis*,*cis* arrangement, usual in related cyclic compounds.[45, 48] The torsional angle between the two diaryl units in the monothiourea **2** is 35.3-38.9º, decreasing almost 70º respect to those present in the bis(thiourea) **1**. The single-crystal X-ray analysis of **2** showed the existence of fourteen independent pairs of racemic molecules in the unit cell, with slightly different shapes. All of them are involved in a complex arrangement interacting by hydrogen bonding.

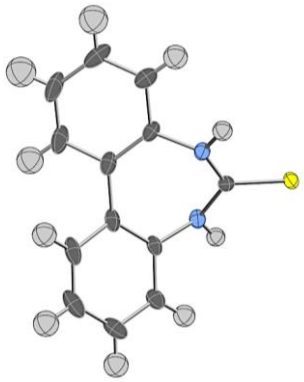

Figure 4 X-Ray structure of the monothiourea **2**. ORTEP drawings with thermal ellipsoids drawn at the 50% probability level.

Finally, crystals of the binaphthyl monothiourea derivative **6** suitable for X-ray analysis were obtained by recrystallization from a $CHCl_3/Et_2O$ mixture (Figure 5). The single-crystal X-ray analysis of **6** shows the existence of one pair of enantiomeric molecules in the unit cell (Supporting Information). The thiourea group is in a *cis*,*cis* arrangement[45, 48] and the torsional angle between the two naphthyl subunits is 48.8º, higher than that of the biphenyl monothiourea **2**.

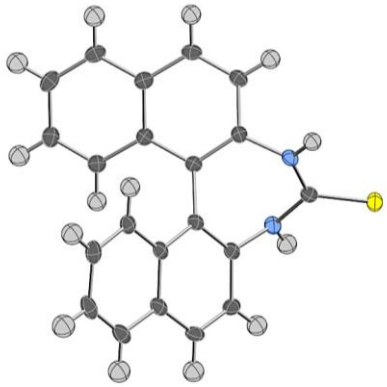

Figure 5 X-Ray structure of the monothiourea **6**. ORTEP drawings with thermal ellipsoids drawn at the 50% probability level.

Study of the Splitting of the Macrocyclic Bis(thioureas) 1 and 8 into Their Respective Monothioureas 2 and 6 in $C_2D_2Cl_4$ and DMF-d_7

To gain insight into the factors involved in the stability of macrocyclic bis(thioureas) **1** and **8** as well as their splitting into their cyclic monothioureas **2** and **6**, these processes were investigated by ^{1}H-NMR spectroscopy in $C_2D_2Cl_4$ and DMF-d_7. A solution of **1** in $C_2D_2Cl_4$ is stable at 25 ºC for three months. However, as time goes by, traces of a highly insoluble solid appears in the NMR tube. The white solid was filtered off and analysed by IR and HRMS (Scheme 4). The IR spectrum is very similar to those of **1** and **2**, showing typical NH bands (3343 and 3119 cm^{-1}). The HRMS shows the base peak at m/z 453.1226 assignable to $[\mathbf{1}\cdot H]^+$. However, another peak at 927.2187, attributable to $[\mathbf{1}\cdot\mathbf{1}\cdot Na]^+$ is also present. The sample was heated until partial solution in $C_2D_2Cl_4$ and then, its ^{1}H NMR was checked. Curiously, the spectrum showed resonances attributable to **3**, **4** and **1**. Considering all the experimental evidences, we assume that the highly insoluble compound corresponds to a mixture of oligomeric structures **9** (Scheme 4, n ≥ 4). Oligomers **9** could be formed by intermolecular coupling of several units of the putative intermediate **10**. Although **10** would be present in undetectable amounts by ^{1}H NMR, the formation of the oligomeric **9** would be driven by its low solubility in $C_2D_2Cl_4$.The reversible nature of the process R-NH-CS-NH-R'⇆R-NH_2 + R'-NCS, would allow the existence of **10** in a certain amount.[49]

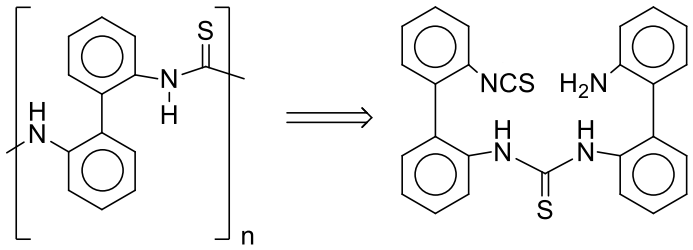

9 **10**

Scheme 4 Structure of the oligomeric compound **9** and the putative intermediate **10**.

The straightforward reversion of the last process in $C_2D_2Cl_4$ became evident from the unexpected conversion of **1** into diamine **3** and bis(isothiocyanate) **4** at 140 ºC for 6 h (left side of Scheme 5, Figure S16). An analogous transformation of the bis(thiourea) **8** into the diamine **5** and bis(isothiocyanate) **7** was observed, but it takes half the time (left side of Scheme 5, Figure S17). In this solvent, the monothiourea **2** can be obtained from **1** at 140 ºC for 35 h (right side of Scheme 5, Figure S18). The same applies to **6**, which is obtained from **8**, although after much longer reaction times (right side of Scheme 5, Figure S19).

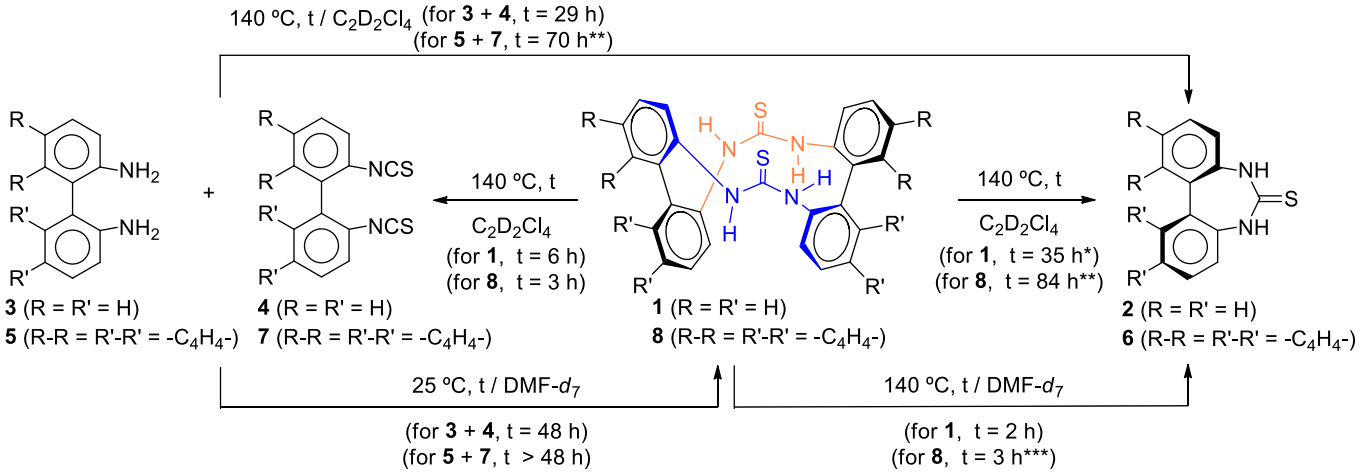

Scheme 5 Evolution of the bis(thioureas) **1** and **8** under different temperatures in $C_2D_2Cl_4$ and DMF-d_7. The reaction of the diamines **3** and **5** with the bis(isothiocyanates) **4** and **7** under different reaction conditions are also included; (*) a small amount of **4** is also observed; (**) only partial formation of **6**, a small amount of **7** is also observed; (***) **5** among other unidentified products also observed.

In $C_2D_2Cl_4$, the bis(thiourea) **1** could not be prepared from **3** and **4** as a single product. Below 120 ºC, the reaction is too slow leading to mixtures of **1** and **2**. By heating at higher temperatures, 140 ºC for 29 h, the reaction led directly to the monothiourea **2** (top part of Scheme 5, Figure S20). Expectedly, the reaction of diamine **5** and bis(isothiocyanate) **7** at 140 ºC led to the monothiourea **6,** but after a longer reaction time (Figure S21).
In DMF-d_7, the course of these processes changes drastically. As expected, **3** and **4** led to the bis(thiourea) **1** as the major product at 25 ºC, even though the formation of monothiourea **2** begins to be detectable after 24 h (bottom part of Scheme 5, Figure S22). Complete conversion of **1** into **2** can be conducted at 60 ºC for 48 h (Figure S23) or at 140 ºC for 2 h. The reaction of binaphthyl derivatives **5** and **7** required a longer time for reaching full conversion into the bis(thiourea) **8** (Figure S24). The conversion of **8** into the monothiourea **6** at 140 ºC is completed in only 3 h (Figure S25).

VT ^{1}H NMR Study of Macrocyclic Bis(thioureas) 1 and 8

To shed further light into the chemical transformation of bis(thioureas) **1** and **8**, VT ^{1}H NMR measurements were conducted in both, $C_2D_2Cl_4$ (230-426 K) and DMF-d_7 (206-426 K). After heating up, a new ^{1}H NMR spectrum was recorded at 313 K for evaluating the extent of decomposition of the corresponding bis(thiourea). The ^{1}H NMR spectra of **1** show well-resolved signals in $C_2D_2Cl_4$ from 230 to 301 K (Figure 6). Above this temperature the resonances broaden until averaged signals are observed above 358 K. The coalescence temperature and the difference in chemical shift between protons H_2 and H_9 ($\Delta\nu$ = 637.5 Hz) allowed the calculation of the activation energy for the *cis*,*trans* ⇆ *trans*,*cis*

switch of the thiourea functions ($\Delta G^{\neq}$ = 16.0 kcal mol^{-1}). The calculated value seems reasonable taking into account that a barrier of 12.8 kcal mol^{-1} has been reported for less strained *N*,*N*'-dialkylthioureas in $CDCl_3$.[50] Starting at 392 K, new resonances are visible in the 6.8-7.0 ppm range, which indicates partial decomposition of the bis(thiourea). The low temperature coefficients ($\Delta\delta/\Delta T$, Figure S26) for NH_1 (+0.7 ppb) and NH_{10} (-1.4 ppb), as well as their low chemical shift values (NH_1: 7.6-7.7 ppm and NH_{10}: 7.2-7.3 ppm) reinforce the presence of non-hydrogen bond aggregates or, in other words, a non-associated bis(thiourea).[51-52] The negligible temperature coefficient of NH_1 agrees with its position inside the cavity, isolated from the bulk solvent.

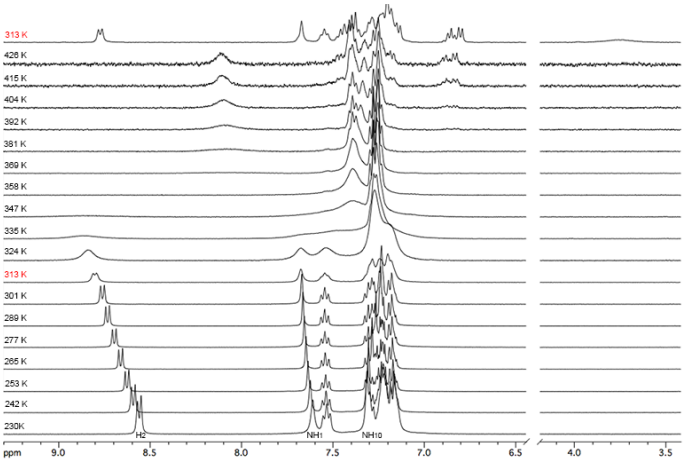

Figure 6 VT ^{1}H NMR spectra of bis(thiourea) **1** in $C_2D_2Cl_4$.

The ^{1}H NMR spectrum of bis(thiourea) **8** in $C_2D_2Cl_4$ shows well-resolved signals from 230 to 335 K (Figure S28). The signals broaden above this temperature. However, no fast exchange regime was observed even when the heating was continued to 426 K. A minimum value for the thiourea-switch activation barrier could be determined from the highest chemical-shift difference between protons H_2 and H_{13} ($\Delta\nu$ = 962.2 Hz) at 426 K, the maximum temperature measured. The $\Delta G^{\neq}$ threshold amounts 18.8 kcal mol^{-1}.[53] Note that exchange processes were observed for both bis(thioureas) in their NOESY spectra which were attributed to the *cis*,*trans* ⇆ *trans*,*cis* switch of both thiourea functions. This fact could be alternatively attributable to the inversion of the twist angle in the biphenyl/binaphthyl subunits. However, this explanation seems to be unlikely, especially for the binaphthyl bis(thiourea) **8**, taking into account that atropisomerization barriers above 35 kcal mol^{-1} has been described for 2,2'-disubstituted binaphthyl derivatives.[54] The control ^{1}H NMR spectrum of **8** recorded at 313 K after heating up to 426 K, shows the almost complete decomposition of the bis(thiourea). In DMF-d_7, the ^{1}H NMR spectra of **1** and **8** were registered in the range of 206-426 K. In the case of bis(thiourea) **1** the broadening of the resonances starts at lower temperatures compared to what occurs in $C_2D_2Cl_4$ (Figure 7). This fact points to a reduced barrier for the thiourea-switch in DMF and it may be rationalized in terms of strong hydrogen bonding between the solvent molecules and the NH groups.[55]

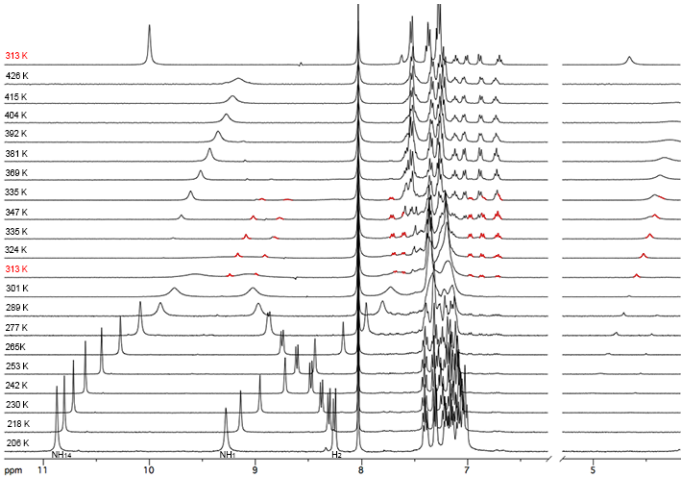

Figure 7 VT ^{1}H NMR spectra of bis(thiourea) **1** in DMF-d_7.

Expectedly, going down to 206-265 K the signals get narrower. The high temperature coefficients, $\Delta\delta/\Delta T$ for NH_1 (-16.4 ppb) and NH_{10} (-11.7 ppb) along with their high chemical shift values (NH_1: 7.7-9.3 ppm and NH_{10}: 9.8-10.9 ppm) seem to confirm the presence of hydrogen bond interactions with the solvent (Figure S27). Signals for the monothiourea **2** and 2,2'-diaminobiphenyl **3** start to emerge in the range of 324-426 K, due to the fast decomposition of the bis(thiourea) **1**. Curiously, low-intensity resonances for an unknown compound rise in the range of 313-335 K (Figure 7, red colour): one broad singlet at 4.4-4.6 ppm, multiplets at 6.7-7.0 ppm and 7.6-7.7 ppm and two broad singlets at 8.7-9.2 ppm. Unfortunately, the structural elucidation of a putative intermediate could not be carried out due to overlapping with other signals, although the broad singlet close to 4.5 ppm suggests a free amino group and the presence of an open intermediate such as **10**. Expectedly, the control ^{1}H NMR spectrum of **1** recorded at 313 K, after heating up, shows the lack of the bis(thiourea) **1** whereas resonances attributed to the monothiourea **2** are neatly present. The behavior of **1** is transferable to its binaphthyl analogous **8** (Figures S30 and S31).

Summarizing the Experimental Study

The above results allow us to reach several conclusions:

1) Both, the formation of the bis(thioureas) **1** and **8** from the respective diamine and bis(isothiocyanate), and their splitting to the corresponding monothioureas take place at much lower temperatures or shorter reaction times in DMF-d_7 compared to $C_2D_2Cl_4$. This fact is probably due to the higher polarity and the basic and good hydrogen-bond acceptor character of the DMF which would stabilize the putative polar transition states.[49]
2) The monothioureas **2** and **6** can be obtained directly from the respective diamine and bis(isothiocyanate) under heating for longer reaction times in DMF-d_7 and $C_2D_2Cl_4$. Thus, while the bis(thioureas) are the kinetically controlled products, the monothioureas are the thermodynamically controlled ones.
3) In the less polar $C_2D_2Cl_4$, the formation of oligomers (**9**) or the cleavage of bis(thioureas) **1** and **8** into the respective diamine and bis(isothiocyanate) are favored (shorter reaction times) when compared to the splitting of each bis(thiourea) into the corresponding monothiourea. The formation of **9** at room temperature would be driven by its low solubility in $C_2D_2Cl_4$. The open intermediate **10** has been proposed to play a key role in these processes in which the reversibility of the equilibrium R-NH-CS-NH-R' ⇆ R-NH_2 + R'-NCS is a key factor.
4) Finally, the change of the biphenyl linkers (**1**) to binaphthyl groups (**8**) favors the opening of the macrocyclic bis(thiourea) into the corresponding diamine and bis(isothiocyanate), probably due to a more strained structure of the corresponding bis(thiourea) with origin in the higher biaryl angle, while disfavors the formation of the corresponding monothiourea, probably by the same reason.

Computational Study

In order to investigate computationally the formation of the bis(thiourea) **1** from the diamine **3** and the bis(isothiocyanate) **4** and its conversion into the monothiourea **2**, we carried out a density functional theory (DFT) study at the B3LYP/6-311+G**//B3LYP/6-31G* theoretical level (for details see Computational Methods in the Supporting Information).

First, we explored the potential energy surface (PES) of this transformation at the gas phase. We found several reaction channels involving a wide variety of processes, such as formation and cleavage of thiourea and isothiourea functions, prototropic equilibria through of 1,3-H sigmatropic shifts, heteroene and retro-heteroene rearrangements, *cis* ⇆ *trans* isomerizations of thiourea functions and, besides, the concurs of crossed paths sharing common stationary points. With the aim of simplifying, we will not present all these findings here, but they can be examined in the Supporting Information. However, after the analysis of these results, and taking into account that 1,3-H sigmatropic shifts play a main role in the mechanistic paths found, we estimated that the transformations under study could be promoted by traces of water present in the reaction mixtures. The precedents of participation of water as "proton switch" in the hydrolysis of *N*-arylureas to give the corresponding isocyanate and amine derivatives also encouraged us to consider this hipothesis.[28, 56] Besides, several computational studies have demonstrated the beneficial effect of considering one water molecule in related hydrogen shifts.[57-59]

The success of water on facilitating the 1,3-H proton transfer is easily understood by considering that, in the lack of water, unimolecular 1,3-H sigmatropic rearrangements would involve four-membered cyclic transition states that are thermally forbidden according with the Woodward-Hoffmann symmetry rules.[60-62] By contrast, the consideration of hydrated complexes enables them to take place through six-membered cyclic transition states involving lower energy barriers (Scheme 6).

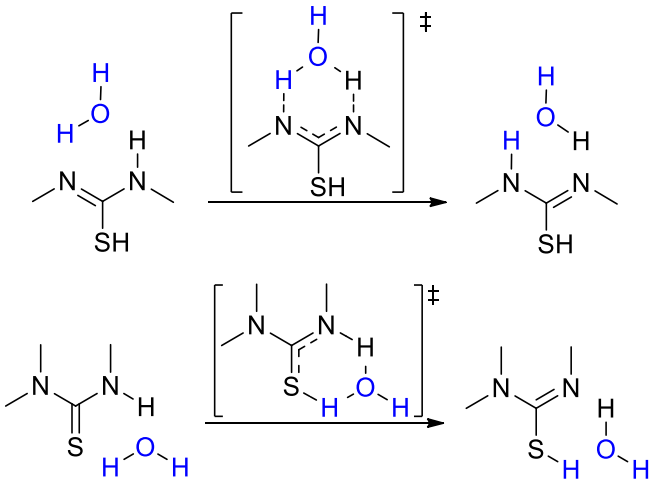

Scheme 6 Water molecule as proton switch assisting the proton transfer between nitrogen atoms (upper) and nitrogen and sulphur atoms (lower) in isothiourea and thiourea functions.

Moreover, the mechanistic paths uncovered at the gas phase involve several stationary points of zwitterionic nature, along with others showing elevated dipolar moment (Table S5, Supporting Information) and, consequently, its formation could be favorably affected by the explicit inclusion of water molecules and the consideration of solvent effects. All these factors could notably alter the energetic profiles of the different paths, or even the reaction mechanisms. Accordingly, we next studied the catalytic influence of one water molecule as proton switch in these processes, firstly at the gas phase and then in DMF as solvent.

The water effect has been analyzed by considering hydrated complexes with one water molecule for both, minima and transition structures connecting them. Due to the complexity of the overall picture, we will only present here a simplified image omitting those paths not competitive for energetic reasons.

The computed Gibbs free energy barriers are depicted in Table 1, where we have also included those corresponding to the study without the participation of water. As presumed, the assistance of water reduces significantly the energy barriers of some key steps, whereas others are slightly increased.

The reaction paths found for the formation of bis(thiourea) **1** and the monothiourea **2** are depicted in Scheme 7, along with the Gibbs free energy barriers computed for each forward (ΔG) and reverse step (ΔG_{-1}) at the gas phase. There are three mechanistic routes (paths ***A-C***) leading to the experimentally isolated thioureas **1** and **2** [from herein we will refer as **1** the bis(thiourea) whose both thiourea functions feature *cis,trans* configuration, as **1*** the bis(thiourea) with one thiourea function showing *trans,trans* configuration and the other *cis,trans,* and as **2** the monothiuorea with *cis,cis* geometry]. To identify the configuration of thiourea functions we use the most extended nomenclature employed for ureas and thioureas.[63] All paths share the first intermediate, besides others that will be discussed later. An overview of each path is described at the bottom of Scheme 7

Table 1. Gibbs free energy barriers[a] for the forward and reverse steps (ΔG and ΔG_{-1}) found in the conversion of 2,2'-diaminobiphenyl (**3**) and bis(isothiocyanato)biphenyl (**4**) into the bis(thiourea) **1** and the monothiourea **2** calculated: i) at the gas phase (B3LYP/6-311++G**//B3LYP/6-31G* theoretical level), ii) taking into consideration the catalytic participation of a water molecule at the gas phase (same level of theory) and iii) in DMF as solvent (SMD-B3LYP/6-31G*/B3LYP/6-31G* theoretical level).

Entry **TS**	**Mechanistic Step**	**ΔG** **ΔG_{-1}**		
		Gas Phase	**H_2O *Gas Phase***	**H_2O DMF**
1 **TS1**	(**3** + **4**) → **11** **N to C addition**	30.9 0.6	33.9 3.4	35.6 8.0
2 **TS2**	**11** → ***trans,cis*-10** **H shift**	17.3 40.5	8.4 29.6	13.2 33.6
3 **TS3a,b**	***trans,cis*-10** → **1***[b] **N to C addition + H shift**	48.6 40.0	29.7 / 16.7 33.8 / 2.0	29.1 / 19.9 35.2 / 7.4
4 **TS5**	***cis,trans*-10**→ **13** **H shift**	42.6 15.9	34.8 8.7	34.5 14.1
5 **TS6**	**13** → 2 **x 14**	0.4 33.6	0.0 23.5	6.0 22.1

	N-C cleavage			
6 **TS7a,b**	**14 → 16**[c] **N to C addition + H shift**	40.8 33.0	17.5 / 13.4 25.5 / 0.1	10.6 / 19.1 23.9/2.8
7 **TS8**	**16→ 2** **H shift**	23.2 39.1	8.5 25.3	10.3 30.0
8 **TS9**	**11 →17** **H shift**	18.9 26.2	12.7 24.2	15.8 20.9
9 **TS10**	**17'→18** **heteroene reaction**	19.3 16.0	20.5 16.7	18.4 19.8
10 **TS11**	**18→19** **H shift**	28.7 39.6	11.7 24.7	12.2 27.6
11 **TS12**	**19→ 14 + 16** **retro-heteroene**	30.3 34.0	31.9 29.9	38.2 29.9
12 **TS13**	***cis,trans*-10 → 17'** **H shift**	33.2 20.2	22.2 7.6	27.9 12.2
13 **TS4**	**1 → 2** **[2+2] / retro [2+2]**	94.5 88.5		
14	ΔG_{rxn} **1**	9.1[d]	9.9[e]	2.7[e]
15	ΔG_{rxn} **2**	-15.0[d]	-13.2[e]	-21.8[e]

[a] Energy barriers in kcal·mol-1. [b] Without the participation of one water molecule this transformation takes place in one step through **TS3** (Supp. Info). [c] Without the participation of one water molecule this transformation takes place in one step through **TS7** (Supp. Info). [d] Gibbs free reaction energy with respect to **3** + **4**. [e] Gibbs free reaction energy with respect to **3** + **4** + H_2O.

First, we located the transition structure **TS1·H_2O** involving the nucleophilic addition of an amino group of the diamine **3** to the carbon atom of one heterocumulene function of the bis(isothiocyanate) **4** leading to the zwitterionic intermediate **11·H_2O**. The computed energy barrier associated to this first step was 33.9 kcal·mol^{-1}.

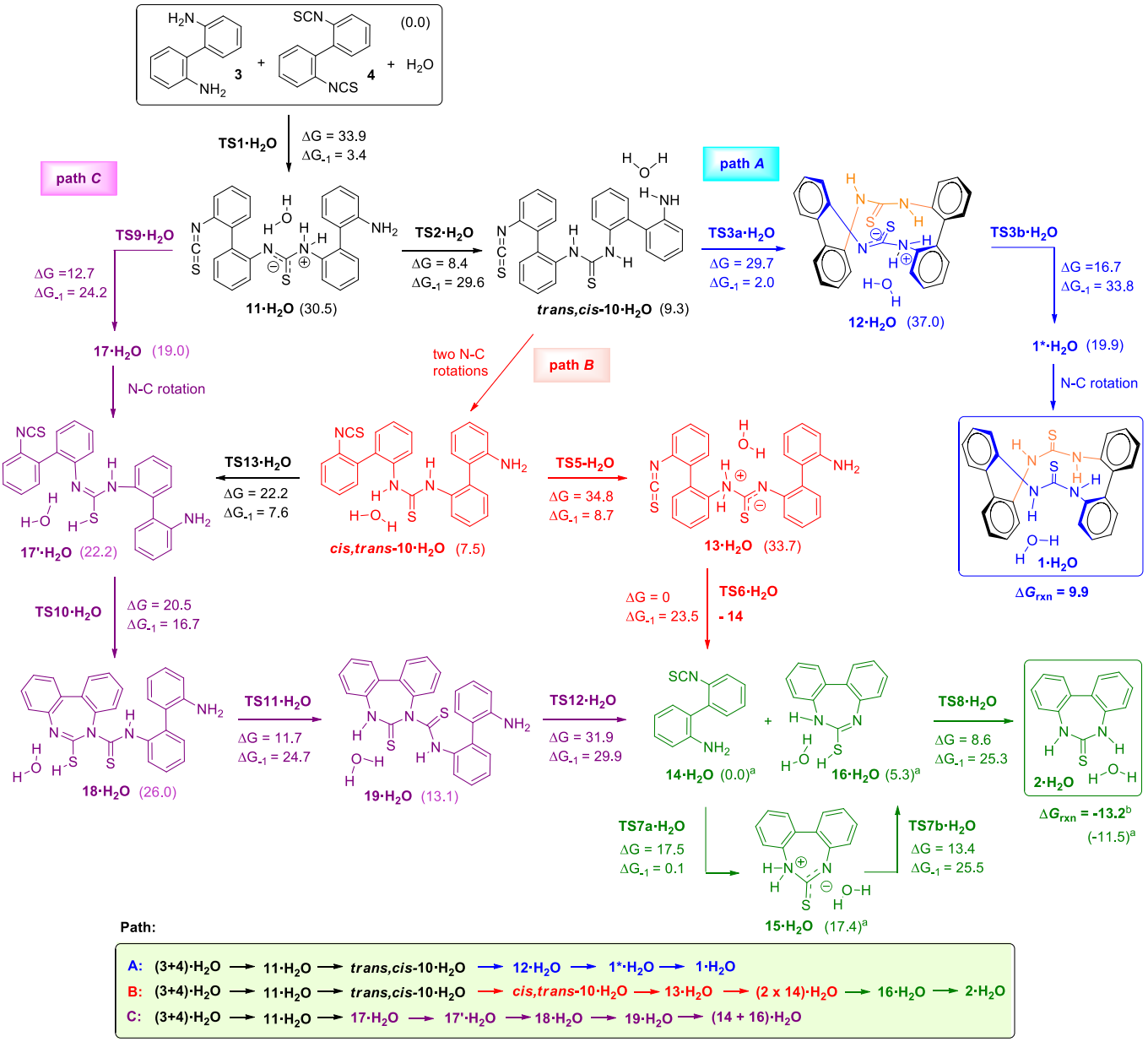

Scheme 7. Mechanistic paths found for the reaction of 2,2'-diaminobiphenyl (**3**) and bis(isothiocyanato)biphenyl (**4**) and its transformation into the bis(thiourea) **1** and the monothiourea **2** by considering the catalytic participation of one water molecule at the gas phase. Gibbs free energy barriers in kcal·mol^{-1} computed at the B3LYP/6-311+G**//B3LYP/6-31G* theoretical level. [a]Energy relative to **14·H$_2$O**. [b]Energy relative to **3** + **4** + **H$_2$O**.

A proton shift from the ammonium group to the negatively charged nitrogen atom transforms **11·H$_2$O** into ***trans,cis*-10·H$_2$O** through the transition structure **TS2·H$_2$O**. The water molecule effectively assists this process via a cyclic six-membered shift showing an easily surmountable energy barrier of 8.4 kcal·mol^{-1}. The intermediate ***trans,cis*-10·H$_2$O** possesses thiourea, amino and isothiocyanate functions allowing its evolution to the bis(thiourea) **1·H$_2$O** and/or to the monothiourea **2·H$_2$O** via paths ***A*** and ***B*** respectively. In consequence, the stationary points **TS2·H$_2$O** and ***trans,cis*-10·H$_2$O** are shared by both paths.

Path ***A*** accounts for the formation of the bis(thiourea) **1·H$_2$O** and involves the construction of the second thiourea function from ***trans,cis*-10·H$_2$O** in two steps through **TS3a·H$_2$O** and, subsequently, **TS3b·H$_2$O**. First, the addition of the nitrogen atom of the amine function to the carbon atom of the isothiocyanate moiety leads to the zwitterionic intermediate **12·H$_2$O**, which in turn through **TS3b·H$_2$O** undergoes proton transfer from the ammonium group to water and from water to the negatively charged nitrogen. This process generates the thioureido function leading to **1*·H$_2$O**. The computed energy barriers for these processes are respectively 29.7 and 16.7 kcal·mol^{-1}. Bis(thiourea) **1*·H$_2$O** differs from the experimentally isolated **1·H$_2$O** in the configuration of one of its thioureido functions and lacks of symmetry elements. Its

conversion into **1·H₂O** involves the rotation of a N-C(=S) bond by surpassing an attainable energy barrier (see Supporting Information for details).
It should be remarked that the direct interconversion of **1** into **2**, that could be reasonably envisaged as resulting from a transannular *trans*-thioureation process (via **TS4**), turned out to be not competitive due to the large value of the associated energy barrier (see Scheme 8 and Supporting Info).

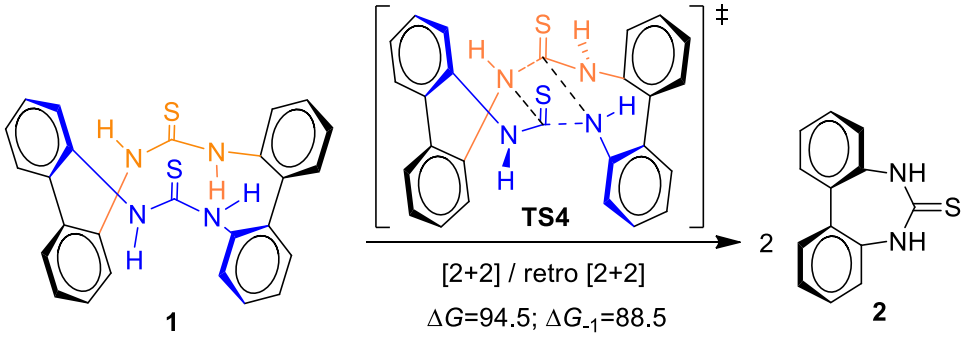

Scheme 8 Direct interconversion between bis(thiourea) **1** and monothiourea **2** via simultaneous [2+2] / retro [2+2] cycloadditions showing the energy barriers computed at the B3LYP/6-311+G**//B3LYP/6-31G* theoretical level.

Path ***B*** connects ***trans,cis*-10·H₂O** to **2·H₂O**. To get started, the intermediate ***trans,cis*-10·H₂O** experiences two consecutive rotations around its N-C thioureido bonds to reach the geometry shown by ***cis,trans*-10·H₂O** (these rotational processes involve low energy barriers, see Supporting Information). Then, this latter species undergoes a water-catalyzed proton shift through **TS5·H₂O** leading to the zwitterionic intermediate **13·H₂O**. The energy barrier associated to this step was computed to be 34.8 kcal·mol^{-1}. The cleavage of the dipolar N-C bond of **13·H₂O**, giving rise to the formation of two molecules of 2-amino-2'-isothiocyanatobiphenyl (**14**), occurs via **TS6·H₂O** without energy barrier (Scheme 7).
Once **14·H₂O** is formed, an intramolecular reaction between their amino and isothiocyanate functions should lead to the monothiourea **2·H₂O**. We found two routes for this process, although only that involving the lowest energy is depicted in Scheme 7. It consists in fact of three consecutive steps: the first one, via **TS7a·H₂O**, involves the addition of the amino group to the isocyanate function resulting in the zwitterion **15·H₂O**. Next this species transfers a proton from the ammonium group to water simultaneously to the shift of a proton from water to the other nitrogen atom through a six-membered cyclic transition structure, via **TS7b·H₂O**, leading to the isothiourea **16·H₂O**. Another subsequent proton transfer assisted by water finally account for its tautomerization into the monothiourea **2·H₂O** via the transition structure **TS8·H₂O**. The energy barriers for these steps have been computed to be 17.5, 13.4 and 8.6 kcal·mol^{-1} respectively.
The third trajectory shown in Scheme 7, path ***C***, constitutes an alternative route to path ***B*** for the formation of the monothiourea **2·H₂O**. It starts from the zwitterionic species **11·H₂O** which, via **TS9·H₂O**, undergoes a proton relocation catalyzed by water from the ammonium group to the nearby sulphur atom leading to the isothioureido intermediate **17·H₂O**. The computed barrier associated to this step is only 12.7 kcal·mol^{-1}. A low-barrier rotation around the N=C isothioureido bond converts **17·H₂O** into its isomer **17'·H₂O** (see Supporting Information).
We were able to locate **TS10·H₂O**, connecting **17'·H₂O** with the intermediate **18·H₂O**, which has a seven-membered isothiourea ring along with thiourea and amino functions. This striking transformation can be seen as an intramolecular heteroene reaction of type I according to the classification of Oppolzer,[64] where the C=S double bond of the isothiocyanate moiety acts as enophile, and the breaking of the H-S bond of the isothioureido function originates a new isothioureido H-S bond between the hydrogen and the sulphur atom of the isothiocyanate fragment. The computed energy barrier for this process is 20.5 kcal·mol^{-1}.
Intermediate **18·H₂O** experiences a proton shift through **TS11·H₂O** leading to its tautomer, the thiourea **19·H₂O**, with an associated energy barrier of 11.7 kcal·mol^{-1}. Such a small value can be attributed again to the catalytic participation of one water molecule. Finally, **19·H₂O** decomposes into a molecule of 2-amino-2'-isothiocyanatobiphenyl (**14·H₂O**) and one of the isothiourea **16·H₂O**. This process, a special type of retro-heteroene reaction, takes place via **TS12·H₂O** involving a computed energy barrier of 31.9 kcal·mol^{-1}. Species **14·H₂O** and **16·H₂O** can evolve through path ***B*** leading to the monothiourea **2**.
As a final point, we also located **TS13·H₂O** connecting paths ***B*** and ***C***, by means of a proton transfer, facilitated again by water, which converts the thioureido intermediate ***cis,trans*-10·H₂O** into the isothiourea **17·H₂O**. The computed energy barrier associated to this mechanistic step is 22.2 kcal·mol^{-1}. It should also be noted that once the intermediate ***cis,trans*-10·H₂O** is formed (the most competitive path for its formation is predicted to be via **11·H₂O** → ***trans,cis*-10·H₂O**), its conversion into **17'·H₂O** via **TS13·H₂O** (path ***C***) is easier than into **13·H₂O** via **TS5·H₂O** (path ***B***) (22.2 *vs* 34.8 kcal·mol^{-1} respectively, see also the reaction profiles shown in Figure 8).

The following points are drawn from the computed energy barriers (forward and reverse) of the mechanistic steps summarized in Scheme 7:

1) The most competitive path accounting for the formation of bis(thiourea) **1** from the reactants is ***A***.
2) Both paths ***B*** and ***C*** result in the formation of monothiourea **2·H₂O** from the starting species.
3) Several routes allow the transformation of bis(thiourea) **1·H₂O** into monothiourea **2·H₂O**, first returning to ***trans,cis*-10·H₂O**, via **TS3b·H₂O** and **TS3a·H₂O**, the highest barrier of the two steps being 33.8 kcal·mol^{-1}. Then, this intermediate could go back to **11·H₂O** surmounting an energy barrier of 29.6 kcal·mol^{-1} for connecting with path ***C***. An alternative way goes by the isomerization of ***trans,cis*-10 H₂O** into ***cis,trans*-10·H₂O** through path ***B*,** or it might transform into **17'·H₂O** passing through **TS13·H₂O** for accessing to path ***C***.
4) The values of Gibbs free energy computed for the formation of **1·H₂O** and **2·H₂O** are 9.9 and -13.2 kcal·mol^{-1} respectively. Consequently, the monothiourea **2·H₂O** is predicted to be the thermodynamically controlled product.

Besides, the main consequences of explicitly considering a water molecule are:

1) The helpfulness of water as proton switch in those steps that involved 1,3-H shifts (entries 2, 4, 7, 8, 10, and 12 in Table 1), now taking place through six-membered cyclic transition states, resulting in a noteworthy decrease of the corresponding energy barriers.
2) The notable decrease in the computed energy barriers of those processes that now consist of two-step sequences (entries 3 and 6).
3) The slight increase of the energy barriers associated to processes whose transition states are merely hydrated complexes (where the water molecule is not playing a significant role, entries 1, 9 and 11).
4) The considerable lowering of energy barriers of those steps corresponding to path ***A*** and ***B*** with respect to without water, while a slight increasing in those of steps **17'·H₂O** → **18·H₂O** and **19·H₂O** → (**14** + **16)·H₂O**, belonging to path ***C***.

Lastly, we studied a mixed model taking into consideration both, the effect of one water molecule and that of DMF as solvent. Thus, the hydrated complexes were introduced into the solvent cavity through the polarizable continuum model SMD. The computed energy barriers values for this approach are summarized in the last column of Table 1, and the energy reaction profiles of the three alternative paths are depicted in Figure 8.

In general, there are not significant changes. As expected, a slight decrease in the energy barriers of most of the steps leading to dipolar intermediates is observed. The greatest lowering (6.9 kcal·mol^{-1}) is found for entry 6, which corresponds to the formation of the intermediate **15·H₂O** from **14·H₂O** (the first step involving **TS7a·H₂O**). By contrast, the barriers of the steps involving a proton shift increase in relation with the gas phase. Reasonably, this increase is greater when the proton shifts lead to a neutral structure from a zwitterionic species, as in entries 2 and 8. It is also worth to note the increase of 6.0 kcal·mol^{-1} observed for the transformation of **13·H₂O** into two units of **14** (entry 5, path ***B***).

When comparing the results for path ***A*** at the gas phase and in DMF, a slight increase in the energy barrier (2.2 kcal·mol^{-1}) for the step **12·H₂O** → **1·H₂O** is produced, and remarkably, now bis(thiourea) **1** is only a little lesser stable than the reactants **3** + **4** (compare the values of ΔG_{rxn} **1** computed at the gas phase and in DMF, 9.9 vs 2.1 kcal·mol^{-1}, entry 14 of Table 1).

For path ***B***, only the increase in the energy barrier of **13·H₂O** → (**14** + **14)·H₂O**, commented above, seems to be significant.

Interestingly, in relation with path ***C***, a lowering of 2.1 kcal·mol^{-1} in the value of the energy barrier can be observed for the heteroene reaction transforming **17'·H₂O** into **18·H₂O** (entry 9), which could be explained on the basis of the high dipolar moment computed for the transition structure **TS10** (Tables S5 and S6 in the Supporting Information). By contrast, it is noteworthy the increase of 6.3 kcal·mol^{-1} for the energy barrier corresponding to the retro-heteroene process **19·H₂O** → (**14** + **16)·H₂O** (31.9 kcal·mol^{-1} at the gas phase *vs* 38.2 kcal·mol^{-1} in DMF, entry 11).

Besides, monothiourea **2** becomes more stable when the solvent effect is taken into account (compare ΔG_{rxn} **2** computed at the gas phase and in DMF, -13.2 vs -21.8 kcal·mol^{-1}, entry 15 of Table 1).

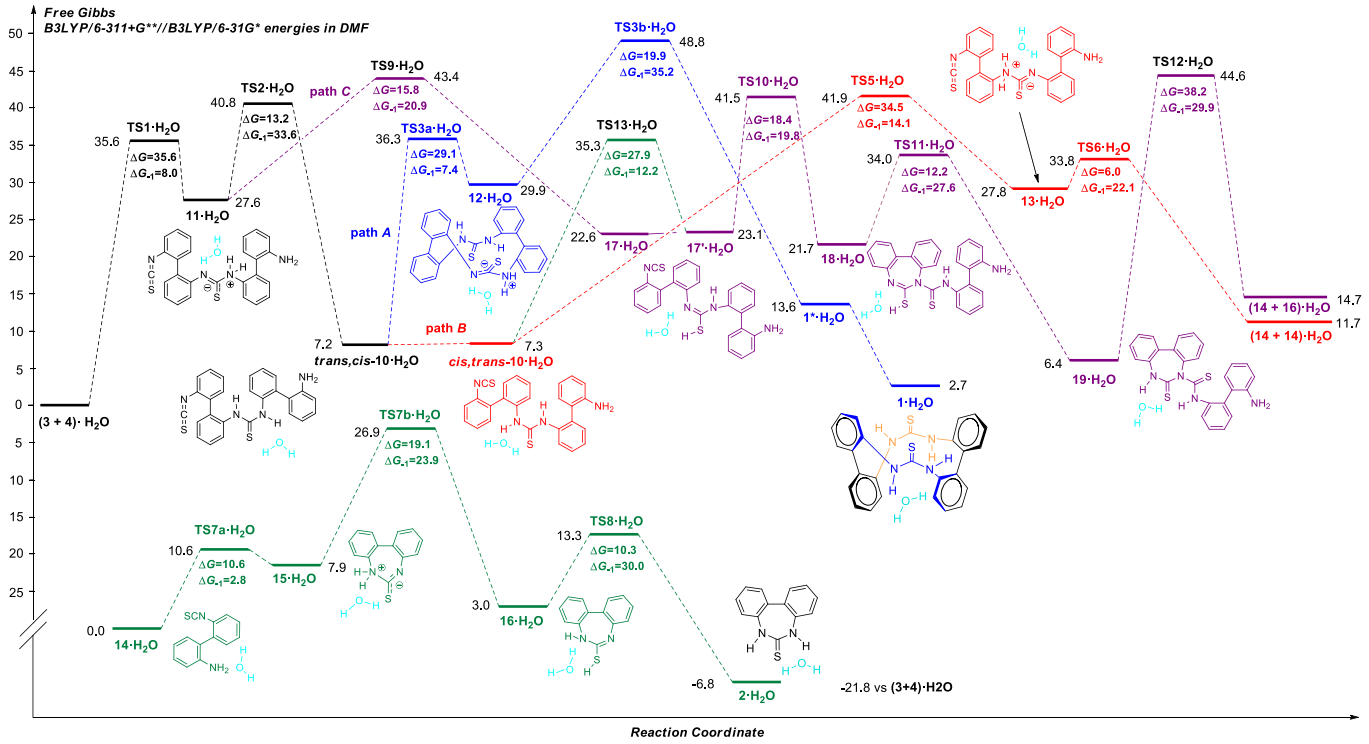

Figure 8. Mechanistic paths found for the reaction of 2,2'-diaminobiphenyl (**3**) and bis(isothiocyanato)biphenyl (**4**) and its transformation into the bis(thiourea) **1** and the monothiourea **2** by considering the catalytic participation of one water molecule in DMF. Gibbs free energy barriers in kcal·mol^{-1} computed at the SMD-B3LYP/6-31G*/B3LYP/6-31G* theoretical level.

As discussed above, the results of our experimental study in DMF suggested that monothiourea **2** would be the thermodynamically controlled product, while bis(thiourea) **1** would be kinetically controlled one. The analysis of the ^{1}H-NMR spectra of the reaction mixture in DMF indicates that a minor quantity of monothiourea **2** is detectable at room temperature after 24 h, endorsing this assumption. Besides, the variation of the **1 : 2** ratio with the reaction time when heating is also in accordance with the hypothesis that bis(thiourea) **1** would be formed as the main product under kinetically controlled reaction conditions. Our computational study agrees with the fact that monothiourea **2** is the thermodynamically controlled product, however, we cannot affirm whether bis (thiourea) **1** is formed at a higher reaction rate than monothiourea **2**. This is due to the existence of the three parallel, crossed and multistep reaction channels ***A-C***, making daring to conjecture whether bis(thiourea) **1** would be the kinetically controlled product. Predicting the evolution over time of the concentration of both products requires a complex kinetic study that is beyond the scope of this paper. Not even the precise identification of the rate-determining states[65,66-71] for each route would allow a non-risky prediction.

Nevertheless, from the results of the whole computational study, we can extract the following conclusions:

1) The mechanistic paths accounting for the formation of bis(thiourea) **1** and monothiourea **2** from **3** and **4** has been elucidated by means of DFT calculations by considering the catalytic participation of one water molecule in both, the gas phase and in DMF as solvent. The complexity of the mechanisms found for these transformations is due to the existence of three alternative paths ***A-C***, each one consisting of multiple steps, but also of crossed routes connecting them.
2) Path ***A*** leads to the formation of bis(thiourea) **1**, whereas paths ***B*** and ***C*** account for the formation of the monothiourea **2**. Additionally, the conversion of bis(thiourea) **1** into monothiourea **2** via a single-step transannular process cannot compete in energetic terms with the alternative multi-step routes.
3) Water acts as an effective proton switch lowering the energy barriers of the steps corresponding to path ***A*** and ***B***, whereas the step with the highest energy barrier among those belonging to path ***C*** increases particularly when the solvent effect of DMF is also considered.
4) Notably, monothiourea **2** is predicted to be the product formed under thermodynamically controlled reaction conditions, in agreement with the experimental study.

Conclusions

Macrocyclic bis(thioureas) with a 14-membered central ring flanked by two 2,2'-biphenylene or 2,2'-binaphthylene fragments can be synthesized by coupling 2,2'-diaminobiaryl and 2,2'-bis(isothiocyanato)biaryl derivatives. The 2,2'-biphenyl and binaphthyl bis(thioureas) show interesting C_2-symmetric twisted structures as revealed by NMR studies and X-ray data. The thioureido function confers to these macrocyclic entities unexpected unstabilities allowing its smooth transformation into either the starting materials used for their preparation or, alternatively, into two molecules of the corresponding monothiourea. Structural factors and solvent polarity play a key role in these latter processes.

The computational study reveals remarkable and unpredicted complex mechanistic routes not only for the formation of the bis(thiourea), but also for its conversion into two units of the cyclic monothiourea, the thermodynamically controlled product. Direct formation of this latter species by other ways not involving the macrocyclic bis(thiourea) also encompasses unexpected intricate paths. Thus, our computational investigation shows the participation of intermediates bearing cyclic and/or acyclic thiourea functions in the mechanistic paths and, more remarkably, the ability of the thiourea group to participate in a wide variety of processes, such as prototropic equilibria through proton shifts, heteroene reactions, retro-heteroene processes, *trans* ⇆ *cis* isomerizations and so forth. This research also brings to light the catalytic participation of a water molecule in these transformations.

As a whole, our study reveals a fascinating combination of reactivity and lability when the thiourea function is incorporated into cyclic scaffolds. Our results might warn further researchers of the incorporation of this function into macrocyclic skeletons bringing out unexpected results, especially if there is a dual kinetic-thermodynamic control of the processes involved in their formation. Moreover, we have also set forth that the reversibility of the reactions between amines and isothiocyanates leading to thioureas is affordable by heating in DMF solution, a fact that could be used in dynamic covalent chemistry for accessing complex molecular assemblies.

Experimental Section

General Experimental Information. HPLC grade solvents (Scharlab) were nitrogen saturated and were dried and deoxygenated using an Innovative Technology Inc. Pure-Solv 400 Solvent Purification System. Column chromatography was carried out using silica gel (60 Å, 70-200 μm, SDS) as stationary phase, and TLC was performed on pre coated silica gel plates with fluorescent indicator 254 nm (Sigma-Aldrich) and observed under UV light. All melting points were determined on a Kofler hot-plate melting point apparatus and are uncorrected. ^{1}H- and ^{13}C{^{1}H}-NMR spectra were recorded at 298 K on a Bruker Avance 300, 400 and 600 MHz instruments. ^{1}H-NMR chemical shifts are reported relative to Me_4Si and were referenced via residual proton resonances of the corresponding deuterated solvent, whereas ^{113}C{^{1}H}-NMR spectra are reported relative to Me_4Si using the carbon signals of the deuterated solvent.

Signals in the ^{1}H- and ^{13}C{^{1}H}-NMR -NMR spectra were assigned with the aid of DEPT-135 or two-dimensional NMR experiments (COSY, ^{1}H,^{1}H-NOESY, HSQC). Abbreviations of coupling patterns are as follows: br, broad; s, singlet; d, doublet; t, triplet; q, quadruplet; m, multiplet. Mass spectra were recorded on a HPLC/MS TOF 6220 mass spectrometer. The PGSE NMR diffusion measurements were performed on a 600 MHz Bruker AVANCE spectrometer, equipped with a microprocessor-controlled gradient unit and a multinuclear inverse probe with an actively shielded Z-gradient coil. The sample was not spun and the airflow was disconnected. The shape of the gradient pulse was rectangular, and its strength varied automatically during the course of the experiments. The *D*-values were determined from the slope of the regression line $\ln(I/I_o)$ *vs* G^2, according to Eq. 1.

$$\ln(I/I_o) = -(\gamma\delta)^2 G^2 (\Delta - \delta/3) D \quad (1)$$

I/I_o = observed spin echo intensity/intensity without gradients, G = gradient strength, Δ = delay between the midpoints of the gradients, D = diffusion coefficient, δ = gradient length.

The calibration of the gradients was carried out via a diffusion measurement of HDO in D_2O ($D_{HDO} = 1.9 \cdot 10^{-9}$ m^2 s^{-1}).[72] The values reported are the average of two different measurements, which yielded *D*-values within max. ± 1.5% of the reported one. All the measurements were carried out using the ^{1}H resonances. The gradient length was set in the range of 1.2 and 1.8 ms and the diffusion delay to ca. 150 ms. D1 was set to $5T_1$. The number of scans was 32 and the experimental time was ca. 90 min. All of the observed data leading to the reported *D*-values afforded lines whose correlation coefficients were above 0.999.

General Computational Information. All stationary points involved in the mechanism of formation of the bis(thiourea) **1** and its transformation into the monothiourea **2** were optimised using the B3LYP functional[73-75] together with the standard 6-31G(d) basis set.[76-79] The optimisations were carried out using the Berny analytical gradient optimisation method[80-81] All structures were characterised by harmonic frequency computations in order to verify that are transition structures or minima in the potential energy surface (PES). The intrinsic reaction coordinate (IRC) paths were traced in order to assess the energy profiles connecting each transition structure (TS) to the two associated minima of the proposed mechanism using the second-order González–Schlegel integration method[82-83] Solvent effects of *N*,*N*-

dimethylformamide (DMF) were taken into account by the polarisable continuum model (PCM) with the Solvation Model based on Density (SMD)[84] in the framework of the self-consistent reaction field (SCRF).[85-87] The values of free Gibbs energies in DMF were calculated with standard statistical thermodynamics at 298.15 K and 1 atm[79] by computing B3LYP/6-311+G** and SMD-B3LYP/6-31G* energies of each stationary point optimized at the B3LYP/6-31G* theoretical level (see Supporting Information for details). All computations were carried out with the Gaussian 09 suite of programs.[88]

Synthesis of the 2,2'-bis(isothiocyanato)binaphthalene (7). The bis(isothiocyanate) **7** was synthesized by the same procedure used in the synthesis of 2,2'-bis(isothiocyanato)biphenyl **4**.[26] The crude product was purified by silica-gel chromatography using 1:9 Et_2O/*n*-hexane as eluent (R_f = 0.6); yield 85%. Spectroscopic data are coincident with those previously reported.[34]

Synthesis of the bis(thiourea) 1. A solution of 2,2'-bis(isothiocyanato)biphenyl[26] **4** (0.44 g, 1.6 mmol) in 45 mL of dry dimethylformamide was added dropwise to a solution of 2,2'-diaminobiphenyl **3** (0.3 g, 1.6 mmol) in 80 mL of the same solvent. The reaction mixture was stirred for 20 h at room temperature. Then, the reaction mixture was poured into water/ice (100 mL). The precipitated solid (0.6 g) was collected by filtration and further purified by silica-gel chromatography (95:5 CH_2Cl_2/Et_2O as eluent, R_f = 0.6); yield 65% (0.48 g); mp 204-206 ºC (colourless prisms, $CHCl_3$/*n*-hexane); ^{1}H NMR ($C_2D_2Cl_4$, 600.13 MHz) δ 7.16-7.18 (m, 2H, H_9), 7.19 (dd, ^3J = 7.8, ^4J = 1.2 Hz, 2H, H_5), 7.23-7.25 (m, 6H, NH_{10} + H_7 + H_8), 7.28-7.29 (m, 2H, H_6), 7.31 (t, ^3J = 7.8 Hz, 2H, H_4), 7.54 (td, ^3J = 7.8, ^4J = 1.2 Hz, 2H, H_3), 7.67 (s, 2H, NH_1), 8.76 (d, ^3J = 8.4 Hz, 2H, H_2); ^{1}H NMR (DMF-d_7, 400.91 MHz) δ 7.15-7.34 (m, 14H), 7.79 (br s, 2H, NH), 8.98 (br s, 2H), 9.87 (br s, 2H, NH); ^{13}C{^{1}H} NMR ($C_2D_2Cl_4$, 100.82 MHz) δ 123.7 (2×CH, C_2), 125.2 (2×CH, C_9), 125.7 (2× CH, C_4), 127.9 (2× CH, C_7 or C_8), 128.85 (2×q), 128.94 (2×CH, C_3), 130.0 (2×CH, C_7 or C_8), 130.3 (2×CH, C_5), 131.7 (2×q), 133.3 (2×q), 133.4 (2×CH, C_6), 135.8 (2×q), 176.7 (2×q, C=S); IR (nujol) 3300, 3156, 1590, 1549, 1508, 1280, 1267, 1178, 768, 760 cm^{-1}; HRMS (ESI) *m/z*: $[M+H]^+$ Calcd for $C_{26}H_{21}N_4S_2$ 453.1202; Found 453.1188.

Synthesis of monothiourea 2. A solution of 2,2'-bis(isothiocyanato)biphenyl **4** (0.22 g, 0.8 mmol) in 25 mL of dry dimethylformamide was added to a solution of 2,2'-diaminobiphenyl **3** (0.15 g, 0.8 mmol) in 20 mL of the same solvent.[26] The reaction mixture was stirred for 20 h at room temperature and then, heated at reflux temperature for 2 h. Then, the reaction mixture was poured into water/ice (80 mL). The precipitated solid was collected by filtration, and subsequently washed with water (3 x 5 mL) and Et_2O (3 x 5 mL). Yield 87% (0.32 g).
The monothiourea **2** can be alternatively prepared in 82% of yield by using a modified method of Le Févre:[33] Carbon disulfide (2.50 g, 32.6 mmol) was added to a solution of 2,2'-diaminobiphenyl **3** (0.40 g, 2.2 mmol) in EtOH (10 mL). The reaction mixture was kept at 80 ºC in a sealed tube for 20 h. After cooling, the yellow needles were filtered out; mp 244-245 ºC (yellow prisms, EtOH). ^{1}H NMR ($C_2D_2Cl_4$, 600.13 MHz) δ 6.92 (dd, ^3J = 7.8, ^4J = 1.2 Hz, 2H, H_2), 7.27 (td, ^3J = 7.7, ^4J = 1.4 Hz, 2H, H_4), 7.32 (td, ^3J = 7.7, ^4J = 1.6 Hz, 2H, H_3), 7.46 (dd, ^3J = 7.5, ^4J = 1.5 Hz, 2H, H_5), 8.01 (s, 2H, NH); ^{13}C{^{1}H} NMR ($C_2D_2Cl_4$, 150.92 MHz) δ 120.9 (2×CH, C_2), 126.3 (2×CH, C_4), 129.1 (2×CH, C_3), 129.67 (2×CH, C_5), 129.68 (2×q), 139.8 (2×q), 193.7 (q, C=S); ^{1}H NMR (DMF-d_7, 400.91 MHz) δ 7.25-7.29 (m, 4H, H_2 + H_4), 7.35-7.39 (m, 2H, H_3), 7.52-7.54 (m, 2H, H_5), 10.10 (br s, 2H, NH); ^{13}C{^{1}H} NMR (DMF-d_7, 100.82 MHz) δ 122.6 (2×CH, C_2), 126.7 (2×CH, C_4), 130.0 (2×CH, C_3), 130.5 (2×CH, C_5), 131.7 (2×q), 142.6 (2×q), 196.2 (q, C=S); IR (nujol) 3231, 3207, 1618, 1559, 1512, 1414, 1283, 1237, 1156, 771, 752, 719, 619 cm^{-1}; HRMS (ESI) *m/z*: $[M+H]^+$ Calcd for $C_{13}H_{11}N_2S$ 227.0637; Found 227.0637.

Synthesis of the monothiourea 6. Carbon disulfide (1.25 g, 16.4 mmol) was added to a solution of 2,2'-diaminobinaphthyl **5** (0.31 g, 1.09 mmol) in EtOH (10 mL). The reaction mixture was kept at 100 ºC in a sealed tube for 24 h. Subsequently, an additional amount (1.25 g, 16.4 mmol) of carbon disulfide was added and the reaction mixture heated at 100 ºC for 24 h more. After cooling, yellow needles crystallized, which were filtered out and washed with EtOH (3 x 5 mL); yield 90% (0.32 g); mp 242-244 ºC (slightly yellow prisms, $CHCl_3$/Et_2O); ^{1}H NMR ($C_2D_2Cl_4$, 600.13 MHz) δ 7.12 (d, ^3J = 8.6 Hz, 2H, H_7), 7.23 (d, ^3J = 9.0 Hz, 2H, H_2), 7.25 (td, ^3J = 7.5 Hz, ^4J = 1.0 Hz, 2H, H_6), 7.47 (t, ^3J = 7.4 Hz, 2H, H_5), 7.92 (d, ^3J = 9.0 Hz, 2H, H_4), 7.93 (d, ^3J = 9.0 Hz, 2H, H_3), 8.00 (s, 2H, NH_1); ^{13}C{^{1}H} NMR ($C_2D_2Cl_4$, 75.45 MHz) δ 120.8 (2×CH, C_2), 123.9 (2×q), 125.6 (2×CH, C_5), 126.6 (2×CH, C_6), 126.9 (2×CH, C_7), 128.1 (2×CH, C_4), 129.9 (2×CH, C_3), 131.5 (2×q), 132.0 (2×q), 140.6 (2×q), 197.1 (q, C=S); ^{1}H NMR (DMF-d_7, 400.91 MHz) δ 7.06 (d, ^3J = 8.5 Hz, 2H, H_7), 7.28 (ddd, ^3J = 8.5, ^3J = 6.9, ^4J = 1.4 Hz, 2H, H_6), 7.49 (ddd, ^3J = 8.1, ^3J = 6.9, ^4J = 1.2 Hz, 2H, H_5), 7.64 (d, ^3J = 8.8 Hz, 2H, H_2), 8.05 (dm, ^3J = 8.4 Hz, 2H, H_4), 8.10 (d, ^3J = 8.9 Hz, 2H, H_3), 10.41 (s, 2H, NH_1); ^{13}C{^{1}H} NMR (DMF-d_7, 100.82 MHz) δ 123.0 (2×CH, C_2), 125.1 (2×q), 126.3 (2×CH, C_5), 127.4 (2×CH, C_6), 127.4 (2×CH, C_7), 129.5 (2×CH, C_4), 130.6 (2×CH, C_3), 132.6 (2×q), 133.2 (2×q), 143.6 (2×q), 198.9 (q, C=S); IR (nujol) 3263, 3193, 1584, 1542, 1320, 1206, 1157, 1142, 816, 806, 787, 756, 727 cm^{-1}; HRMS (ESI) *m/z*: $[M+H]^+$ Calcd for $C_{21}H_{15}N_2S$ 327.0956; Found 327.0944.

Synthesis of the bis(thiourea) 8. A solution of 2,2'-bis(isothiocyanato)binaphthyl **7** (0.44 g, 1.2 mmol) in 40 mL of dry dimethylformamide was added dropwise at 0 ºC for 2 h to a solution of 2,2'-diaminobinaphthyl **5** (0.34 g, 1.2 mmol) in 60 mL of the same solvent. The reaction mixture was stirred for 20 h more at room temperature. Then, the reaction mixture was poured into water/ice. The precipitated solid (0.6 g) was collected by filtration, washed with water, and air-dried. The crude product was further purified by silica-gel chromatography by using 9.5:0.5 CH_2Cl_2/Et_2O as eluent (R_f = 0.7); yield 61% (0.48 g); mp 225-227 ºC (slightly yellow prisms, $CHCl_3$/*n*-hexane); ^{1}H NMR ($C_2D_2Cl_4$, 600.13 MHz) δ 6.72 (dd, ^3J = 8.5, ^4J =0.7 Hz, 2H, H_7), 6.87 (d, ^3J = 8.7 Hz, 2H, H_{12}), 6.90 (d, ^3J = 8.7 Hz, 2H, H_{13}), 6.96 (s, 2H, NH_{14}), 6.97 (d, ^3J = 8.4 Hz, 2H, H_8), 7.20 (ddd, ^3J = 8.4, ^3J = 7.0, ^4J = 1.3 Hz, 2H, H_6), 7.43-7.46 (m, 4H, H_5 + H_9) 7.58 (s, 2H, NH_1), 7.71 (ddd, ^3J = 8.1, ^3J = 6.9, ^4J = 1.1 Hz, 2H, H_{10}), 7.76 (d, ^3J = 8.0 Hz, 2H, H_{11}), 7.97 (d, ^3J = 8.2 Hz, 2H, H_4), 8.08 (d, ^3J = 9.2 Hz, 2H, H_3), 9.30 (d, ^3J = 9.2 Hz, 2H, H_2); ^{13}C{^{1}H} NMR ($C_2D_2Cl_4$, 150.92 MHz) δ 120.1 (2×q), 120.9 (2×CH, C_2), 122.7 (2×CH, C_{13}), 124.5 (2×CH, C_7), 125.6 (4×CH, C_8 + C_5 or C_9), 127.0 (2×q), 127.15 (2×CH, C_6 or C_{10}), 127.17 (2×CH, C_6 or C_{10}), 128.2 (2×CH, C_5 or C_9), 128.5 (2×CH, C_4), 128.7 (2×CH, C_{11}), 129.1 (2×CH, C_3), 130.1 (2×CH, C_{12}), 130.9 (2×q), 131.9 (2×q), 132.0 (2×q), 132.2 (2×q), 133.4 (2×q), 135.1 (2×q), 177.1 (2×q, C=S); ^{1}H NMR (DMF-d_7, 400.91 MHz) δ 6.66 (d, ^3J = 8.4 Hz, 2H, H_7), 6.90-6.93 (m, 4H, H_8 + H_{13}), 7.02 (d, ^3J = 8.8 Hz, 2H, H_{12}), 7.17 (ddd, ^3J = 8.3, ^3J = 7.2, ^4J = 1.0 Hz, 2H, H_6), 7.39-7.43 (m, 4H, H_5 + NH_1), 7.53 (tm, ^3J = 8.0 Hz, 2H, H_9), 7.80 (tm, ^3J = 7.5 Hz, 2H, H_{10}), 7.98-8.03 (m, 4H, H_4 + H_{11}), 8.10 (d, ^3J = 9.2 Hz, 2H, H_3), 9.76 (d, ^3J = 9.2 Hz, 2H, H_2), 10.02 (s, 2H, NH_{14}); ^{13}C{^{1}H} NMR (DMF-d_7, 100.82 MHz) δ 120.7 (2×CH, C_2), 121.6 (2×q), 125.78 (2×CH, C_8 or C_{13}), 125.82 (2×CH, C_5), 126.4 (2×CH, C_8 or C_{13}), 126.8 (2×CH, C_7), 127.4 (2×CH, C_6), 128.4 (2×CH, C_{10}), 128.9 (2×CH, C_4), 129.0 (2×CH, C_3), 129.1 (2×CH, C_9), 130.3 (2×q), 130.7 (2×CH, C_{11}), 131.5 (2×CH, C_{12}), 131.6 (2×q), 133.8 (2×q), 134.0 (2×q), 134.5 (2×q), 134.8 (2×q), 137.1 (2×q), 178.4 (2×q, C=S); IR (nujol) 3379, 3324, 1599, 1537, 1318, 1240, 1179, 819, 750 cm^{-1}; HRMS (ESI) *m/z*: $[M+H]^+$ Calcd for $C_{42}H_{29}N_4S_2$ 653.1824; Found 653.1831.

Associate Content

Supporting Information

The Supporting Information is available free of charge on the ACS Publications website at DOI: xxx

Crystal data for compounds **1**, **2** and **6** (CIF). CCDC 1810754, 1810755 and 1810756.

X-Ray ORTEP figures, NMR and computational data (pdf).

Acknowledgements

This work was supported by the *MINECO* (Project CTQ2017-87231-P) and the *Fundación Seneca-CARM* (Project 19240/PI/14). We also are grateful to Dr. M. Marin-Luna for their useful comments on the solvent effects calculations.

Notes and references

1. Ren, J.; Diprose, J.; Warren, J.; Esnouf, R. M.; Bird, L. E.; Ikemizu, S.; Slater, M.; Milton, J.; Balzarini, J.; Stuart, D. I.; Stammers, D. K., Phenylehylthiazolylthiourea (PETT) Non-nucleoside Inhibitors of HIV-1 and HIV-2 Reverse Transcriptases. *J. Biol. Chem.* **2000,** *275*, 5633-5639.

2. Rodríguez-Fernández, E.; Manzano, J. L.; Benito, J. J.; Hermosa, R.; Monte, E.; Criado, J. J., Thiourea, Triazole and Thiadiazine Compounds and Their Metal Complexes as Antifungal Agents. *J. Inorg. Biochem.* **2005,** *99*, 1558-1572.

3. Stefanska, J.; Szulczyk, D.; Koziol, A. E.; Miroslaw, B.; Kedzierska, E.; Fidecka, S.; Busonera, B.; Sanna, G.; Giliberti, G.; La Colla, P.; Struga, M., Disubstituted Thiourea Derivatives and Their Activity on CNS: Synthesis and Biological Evaluation. *Eur. J. Med. Chem.* **2012,** *55*, 205-213.

4. Saeed, A.; Florke, U.; Erben, M. F., A Review on the Chemistry, Coordination, Structure and Biological Properties of 1-(Acyl/Aroyl)-3(substituted) Thioureas. *J. Sulfur Chem.* **2013,** *35*, 318-355.

5. Yun, T.; Qin, T.; Liu, Y.; Lai, L., Identification of Acylthiourea Derivatives as Potent Plk1 PBD Inhibitors. *Eur. J. Med. Chem.* **2016,** *124*, 229-236.

6. Dalecki, A. G.; Malalasekera, A. P.; Schaaf, K.; Kutsch, O.; Bossmann, S. H.; Wolschendorf, F., Combinatorial Phenotypic Screen Uncovers Unrecognized Family of Extended Thiourea Inhibitors with Copper-Dependent Anti-Staphylococcal Activity. *Metallomics* **2016,** *8*, 412-421.

7. Bregovic, V. B.; Basaric, N.; Mlinaric-Majerski, K., Anion Binding with Urea and Thiourea Derivatives. *Coord. Chem. Rev.* **2015,** *295*, 80-124.

8. Doyle, A. G.; Jacobsen, E. N., Small-Molecule H-Bond Donors in Asymmetric Catalysis. *Chem. Rev.* **2007,** *107*, 5713-5743.

9. Takemoto, Y., Development of Chiral Thiourea Catalysts and Its Application to Asymmetric Catalytic Reactions. *Chem. Pharm. Bull.* **2010,** *58*, 593-601.

10. Fang, X.; Wang, C.-J., Recent Advances in Asymmetric Organocatalysis Mediated by Bifunctional Amine-Thioureas Bearing Multiple Hydrogen-Bonding Donors. *Chem. Commun.* **2015,** *51*, 1185-1197.

11. Zhang, Y.; Liu, Y.-K.; Kang, T.-R.; Hu, Z.-K.; Chen, Y.-C., Organocatalytic Enantioselective Mannich-Type Reaction of Phosphorus Ylides: Synthesis of Chiral N-Boc-beta-Amino-alfa-methylene Carboxylic Esters. *J. Am. Chem. Soc.* **2008,** *130*, 2456-2457.
12. Tan, B.; Hernandez-Torres, G.; Barbas III, C. F., Highly Efficient Hydrogen-Bonding Catalysis of the Diels-Alder Reaction of 3-Vinylindoles and Methyleneindolinones Provides Carbazolespirooxindole Skeletons. *J. Am. Chem. Soc.* **2011,** *133*, 12354-12357.
13. Sohtome, Y.; Nagasawa, K., Dynamic Asymmetric Organocatalysis: Cooperative Effects of Weak Interactions and Conformational Flexibility in Asymmetric Organocatalysts. *Chem. Commun.* **2012,** *48*, 7777-7789.
14. Shi, M.; Liu, X.-G., Asymmetric Morita-Baylis-Hillman Reaction of Arylaldehydes with 2-Cyclohexen-1-one Catalyzed by Chiral Bis(Thio)urea and DABCO. *Org. Lett.* **2008,** *10*, 1043-1046.
15. Tobe, Y.; Sasaki, S.-i.; Hirose, K.; Naemura, K., Novel Self-Assembly of m-Xylylene Type Dithioureas. *Tetrahedron Lett.* **1997,** *38*, 4791-4794.
16. Custelcean, R., Crystal Engineering with Urea and Thiourea Hydrogen-Bonding Groups. *Chem. Commun.* **2008**, 295-307.
17. Paisner, K.; Zakharov, L. N.; Doxsee, K. M., A Robust Thiourea Synthon for Crystal Engineering. *Cryst. Growth Des.* **2010,** *10*, 3757-3762.
18. Silva, A. L. R.; Ribeiro da Silva, M. D. M. C., Comprehensive Thermochemical Study of Cyclic Five- and Six- Membered N,N'-Thioureas. *J. Chem. Eng. Data* **2017,** *62*, 2584-2591.
19. Irngartinger, V. H., Kristall- und Molekularstruktur des chiralen Hexa-o-phenylens. *Acta Cryst.* **1973,** *B29*, 894-902.
20. Tauer, E.; Grellmann, K.-H.; Heinrich, A., Photochemistry of Tetrabenzo[c,e,i,k][1,2,7,8]tetraazacyclododecine in 2-Propanol. *Chem. Ber.* **1991,** *124*, 2053-2055.
21. Tauer, E.; Grellmann, K.-H.; Heinrich, A., Photochemistry of di-Schiff Bases and Related Compounds. *Liebigs Ann.* **1995**, 657-660.
22. Temma, T.; Kobayashi, M.; Agata, Y.; Yamane, T.; Miura, J., Syntheses of Helical Polymers through the Combination of Axially Dissymmetric Segments. *J. Polym. Sci., Part A: Polym. Chem.* **2004,** *42*, 4607-4620.
23. Staab, H. A.; Wehinger, E., Synthesis of 9,10, 19, 20,-Tetradehydrotetrabenzo[acgi]cyclodecene. *Angew. Chem. Int. Ed.* **1968,** *7*, 225-226.
24. Imgartinger, H., Intramolecular Interactions between Triple Bonds. XV. Crystal and Molecular Structure of 9,10,19,20-Tetradehydrotetrabenz[a,c,g,i]cyclododecene as Adduct with Benzene. *Chem. Ber.* **1973,** *106*, 761-772.
25. Toyota, S.; Kawai, K.; Iwanaga, T.; Wakamatsu, K., Tolanophane Revisited-Resolution and Racemization Mechanism of a Twisted Chiral Aromatic Compound. *Eur. J. Org. Chem.* **2012**, 5679-5684.
26. Alajarin, M.; Molina, P.; Sanchez-Andrada, P.; Foces-Foces, M. C., Preparation and Intramolecular Cyclization of Bis(carbodiimides). Synthesis and X-ray Structure of 1,3-Diazetidine-2,4-diimine Derivatives. *J. Org. Chem.* **1999,** *64*, 1121-1130.
27. Watts, A. S.; Gavalas, V. G.; Cammers, A.; Sanchez-Andrada, P.; Alajarin, M.; Bachas, L. G., Nitrate-Selective Electrode Based on a Cyclic bis-Thiourea Ionophore. *Sens. Actuators, B* **2007,** *121*, 200-207.
28. Giffney, C. J.; O'Connor, C. J., Hydrolysis of Phenylureas. Part II. Hydrolysis in Acid and Aqueous Solutions. *J. Chem. Soc. Perkin Trans. 2* **1976**, 362-368.
29. Mollett, K. J.; O'Connor, C. J., Hydrolysis of Phenylureas. Part III. Micellar Effects on the Solubilization and Decomposition of 4-Methyl- and 4-Nitro-phenylurea. *J. Chem. Soc. Perkin Trans. 2* **1976**, 369-374.
30. Laudien, R.; Mitzner, R., Phenylureas. Part 1. Mechanism of the Basic Hydrolysis of Phenylureas. *J. Chem. Soc. Perkin Trans. 2* **2001**, 2226-2229.
31. Laudien, R.; Mitzner, R., Phenylureas. Part 2. Mechanism of the Acid Hydrolysis of Phenylureas. *J. Chem. Soc. Perkin Trans. 2* **2001**, 2230-2232.
32. Salvestrini, S.; Di Cerbo, P.; Capasso, S., Kinetics and Mechanism of Hydrolysis of Phenylureas. *J. Chem. Soc. Perkin Trans. 2* **2002**, 1889-1893.
33. Le Fèvre, R. J. W., Corrections in the Chemistry of Diphenyl Derivatives of the "Kaufler" Type, and the Formation of Dibenzoctdiazines. *J. Chem. Soc.* **1929**, 733-738.
34. Atzrodt, J.; Beckert, R.; Darsen, A., Synthesis of New Axial Chiral Diisothiocyanates. *Tetrahedron: Asymmetry* **1997,** *8*, 2257-2260.
35. Their NMR spectra were initially measured in deuterated DMSO in order to be compared with those previously reported. Nevertheless for a more thorough study, we decided to change to DMF and tetrachloroethane due to the extremely low solubility of the compounds.
36. Although the mechanisms of chemical exchange and the NOE are quite unrelated, they share in common the transfer of longitudinal magnetisation and as such can be detected in the same 2D NMR experiment.
37. Pastor, A.; Martinez-Viviente, E., NMR Spectroscopy in Coordination Supramolecular Chemistry: A Unique and Powerful Methodology. *Coord. Chem. Rev.* **2008,** *252*, 2314-2345.
38. Jeener, J.; Meier, B. H.; Bachmann, P.; Ernst, R. R., Investigation of Exchange Processes by Two-Dimensional NMR Spectroscopy. *J. Chem. Phys.* **1979,** *71*, 4546-4553.
39. Rampalakos, C.; Wulff, W. D., A Novel Bis-Thiourea Organocatalyst for the Asymmetric Aza-Henry Reaction. *Adv. Synth. Catal.* **2008,** *350*, 1785-1790.
40. Stejskal, E. O.; Tanner, J. E., Spin Diffusion Measurements: Spin Echoes in the Presence of a Time-Dependent Field Gradient. *J. Chem. Phys.* **1965,** *42*, 288-292.
41. Johnson Jr., C. S., Diffusion Ordered Nuclear Magnetic Resonance Spectroscopy: Principles and Applications. *Prog. Nucl. Magn. Reson. Spectrosc.* **1999,** *34*, 203-256.
42. Cohen, Y.; Avram, L.; Frish, L., Diffusion NMR Spectroscopy in Supramolecular and Combinatorial Chemistry: an Old Parameter-New Insights. *Angew. Chem. Int. Ed.* **2005,** *44*, 520-554.
43. Alajarin, M.; Pastor, A.; Orenes, R.-A.; Martinez-Viviente, E.; Pregosin, P. S., Pulsed Gradient Spin Echo (PGSE) Diffusion Measurements as a Tool for the Elucidation of a New Type of Hydrogen-Bonded Bicapsular Aggregate. *Chem. Eur. J.* **2006,** *12*, 877-886.
44. Sisco, S. W.; Moore, J. S., Homochiral self-Sorting of BINOL Macrocycles. *Chem. Sci.* **2014,** *5*, 81-85.

45. Custelcean, R.; Gorbunova, M. G.; Bonnesen, P. V., Steric Control over Hydrogen Bonding in Crystalline Organic Solids: A Structural Study of N,N'-Dialkylthioureas. *Chem. Eur. J.* **2005,** *11*, 1459-1466.
46. Chong, Y. S.; Carroll, W. R.; Burns, W. G.; Smith, M. D.; Shimizu, K. D., A High-Barrier Molecular Balance for Studying Face-to-Face Arene-Arene Interactions in the Solid State and in Solution. *Chem. Eur. J.* **2009,** *15*, 9117-9126.
47. Surange, S. S.; Kumaran, G.; Rajappa, S.; Pal, D.; Chakrabarti, P., Push-Pull Butadienes: Evidence for a Possible C-H···S Hydrogen Bond in 4-(Methylthio)-4-nitro-1-(pyrrolidin-1-yl)buta-1,3-diene. *Helv. Chim. Acta* **1997,** *80*, 2329-2336.
48. McBride, M. T.; Luo, T.-J. M.; Palmore, G. T. R., Hydrogen-Bonding Interactions in Crystalline Solids of Cyclic Thioureas. *Cryst. Growth Des.* **2001,** *1*, 39-46.
49. Vanassche, W.; Hoornaert, G., Study of the Kinetics, Intermediates and Product Distribution in the Synthesis and Decomposition Reactions of Thiourea Derivatives. *Bull. Soc. Chim. Belges* **1971,** *80*, 505-520.
50. Rang, K.; Sandström, J.; Svensson, C., The Conformational Equilibrium of N,N'-Bis-[(S)-1-phenylethyl]-thiourea and Its Solvent Dependence, Studied by NMR and CD Spectra and by X-ray Crystallography. *Can. J. Chem.* **1998,** *76*, 811-820.
51. Belvisi, L.; Gennari, C.; Mielgo, A.; Potenza, D.; Scolastico, C., Conformational Preferences of Peptides Containing Reverse-Turn Mimetic Bicyclic Lactams: Inverse gamma-Turns versus Type-II' beta-Turns-Insights into beta-Hairpin Stability. *Eur. J. Org. Chem.* **1999**, 389-400.
52. Stevens, E. S.; Sugawara, N.; Bonora, G. M.; Toniolo, C., Conformational Analysis of Linear Peptides. Temperature Dependence of NH Chemical Shifts in Chloroform. *J. Am. Chem. Soc.* **1980,** *102*, 7048-7050.
53. Rotzler, J.; Gsellinger, H.; Bihlmeier, A.; Gantenbein, M.; Vonlanthen, D.; Häussinger, D.; Klopper, W.; Mayor, M., Atropisomerization of Di-para-substituted Propyl-bridged Biphenyl Cyclophanes. *Org. Biomol. Chem.* **2013,** *11*, 110-118.
54. Bringmann, G.; Mortimer, A. J. P.; Keller, P. A.; Gresser, M. J.; Garner, J.; Breuning, M., Atroposelective Synthesis of Axially Chiral Biaryl Compounds. *Angew. Chem. Int. Ed.* **2005,** *44*, 5384-5427.
55. Isaksson, G.; Sandström, J., Barriers to Internal Rotation, Ultraviolet Spectra, and Conformations of N,N-Dimethyl-N'-arylthioureas and N,N,N'-Trimethylthioureas. *Acta Chem. Scand.* **1970,** *24*, 2565-2582.
56. Hutchby, M.; Houlden, C. E.; Ford, J. G.; Tyler, S. N. G.; Gagné, M. R.; Lloyd-Jones, G. C.; Booker-Milburn, K. I., Hindered Ureas as Masked Isocyanates: Facile Carbamoylation of Nucleophiles under Neutral Conditions. *Angew. Chem. Int. Ed.* **2009,** *48*, 8721-8724.
57. Trujillo, C.; Sanchez-Sanz, G.; Alkorta, I.; Elguero, J., A Theoretical Investigation of the Mechanism of Formation of a Simplified Analog of the Green Fluorescent Protein (GFP) from a Peptide Model. *Struct. Chem.* **2013,** *24*, 1145-1151.
58. Azofra, L. M.; Alkorta, I.; Elguero, J.; Toro-Labbé, A., Mechanisms of Formation of Hemiacetals: Intrinsic Reactivity Analysis. *J. Phys. Chem. A* **2012,** *116*, 8250-8259.
59. Markova, N.; Enchev, V.; Timtcheva, I., Oxo-Hydroxy Tautomerism of 5-Fluorouracil: Water-Assisted Proton Transfer. *J. Phys. Chem. A* **2005,** *109*, 1981-1988.
60. Woodward, R. B.; Hoffmann, R., Stereochemistry of Electrocyclic Reactions. *J. Am. Chem. Soc.* **1965,** *87*, 395-397.
61. Hoffmann, R.; Woodward, R. B., Selection Rules for Concerted Cycloaddition Reactions. *J. Am. Chem. Soc.* **1965,** *87*, 2046-2048.
62. Woodward, R. B.; Hoffmann, R., The Conservation of Orbital Symmetry. *Angew. Chem. Int. Ed. Engl.* **1969,** *8*, 781-853.
63. Yamasaki, R.; Iida, M.; Ito, A.; Fukuda, K.; Tanatani, A.; Kagechika, H.; Masu, H.; Okamoto, I., Crystal Engineering of N,N'-Diphenylurea Compounds Featuring Phenyl–Perfluorophenyl Interaction. *Cryst. Growth Des.* **2017,** *17*, 5858-5866.
64. Oppolzer, W.; Snieckus, V., Intramolecular Ene Reactions in Organic Synthesis. *Angew. Chem. Int. Ed. Engl.* **1978,** *17*, 476-486.
65. The rate-determining states can be defined as the transition state and the intermediate exerting the strongest effect on the overall rate with a differential change on their Gibbs energies. For references dealing with appropriated managing of these concepts see refs 66-71.
66. Kozuch, S.; Martin, J. M. L., The Rate-Determining Step is Dead. Long Live the Rate-Determining State! *Chem. Phys. Chem.* **2011,** *12*, 1413-1418.
67. Meek, S. J.; Pitman, C. L.; Miller, A. J. M., Deducing Reaction Mechanism: A Guide for Students, Researchers, and Instructors. *J. Chem. Educ.* **2016,** *93*, 275-286.
68. Laidler, K. J., Rate-Controlling Step: A Necessary or Useful Concept? *J. Chem. Educ.* **1988,** *65*, 250-254.
69. Murdoch, J. R., What is the Rate-Limiting Step of a Multistep Reaction? *J. Chem. Educ.* **1981,** *58*, 32-36.
70. Kozuch, S.; Shaik, S., How to Conceptualize Catalytic Cycles? The Energetic Span Model. *Acc. Chem. Res.* **2011,** *44*, 101-110.
71. Campbell, C. T., The Degree of Rate Control: A Powerful Tool for Catalysis Research. *ACS catal.* **2017,** *7*, 2770-2779.
72. Holz, M.; Weingärtner, H., Calibration in Accurate Spin-Echo Self-Diffusion Measurements Using 1H and Less-Common Nuclei. *J. Magn. Reson.* **1991,** *92*, 115-125.
73. Lee, C.; Yang, W.; Parr, R. G., Development of the Colle-Salvetti Correlation-energy Formula into a Functional of the Electron Density. *Phys. Rev. B* **1988,** *37*, 785-789.
74. Becke, A. D., Density-functional Exchange-energy Approximation with Correct Asymptotic Behavior. *Phys. Rev. A* **1988,** *38*, 3098-3100.
75. Stephens, P. J.; Devlin, F. J.; Chabalowski, C. F.; Frisch, M. J., Ab Initio Calculation of Vibrational Absorption and Circular Dichroism Spectra Using Density Functional Force Fields. *J. Phys. Chem.* **1994,** *98*, 11623-11627.
76. Becke, A. D., Density-functional Thermochemistry. III. The Role of Exact Exchange. *J. Chem. Phys.* **1993,** *98*, 5648-5652.
77. Krishnan, R.; Binkley, J. S.; Seeger, R.; Pople, J. A., Self-consistent Molecular Orbital Methods. XX. A Basis Set for Correlated Wave Functions. *J. Chem. Phys.* **1980,** *72*, 650-654.
78. Gill, P. M. W.; Johnson, B. G.; Pople, J. A.; Frisch, M. J., The Performance of the Becke—Lee—Yang—Parr (B—LYP) Density Functional Theory with Various Basis Sets. *Chem. Phys. Lett.* **1992,** *197*, 499-505.
79. Hehre, W. J.; Radom, L.; Schleyer, P. v. R.; Pople, J. A., *Ab Initio Molecular Orbital Theory*. Wiley: New York, 1986.
80. Schlegel, H. B., Optimization of Equilibrium Geometries and Transition Structures. *J. Comput. Chem.* **1982,** *3*, 214-218.
81. Schlegel, H. B., *Modern Electronic Structure Theory*. World Scientific: Singapore, 1995; p 459-500.
82. Gonzalez, C.; Schlegel, H. B., Reaction Path Following in Mass-Weighted Internal Coordinates. *J. Phys. Chem.* **1990,** *94*, 5523-5527.

83. Gonzalez, C.; Schlegel, H. B., Improved Algorithms for Reaction Path Following: Higher-order Implicit Algorithms. *J. Chem. Phys.* **1991,** *95*, 5853-5860.
84. Marenich, A. V.; Cramer, C. J.; Truhlar, D. G., Universal Solvation Model Based on Solute Electron Density and on a Continuum Model of the Solvent Defined by the Bulk Dielectric Constant and Atomic Surface Tensions. *J. Phys. Chem. B* **2009,** *113*, 6378-6396.
85. Cances, E.; Mennucci, B.; Tomasi, J., A New Integral Equation Formalism for the Polarizable Continuum Model: Theoretical Background and Applications to Isotropic and Anisotropic Dielectrics. *J. Chem. Phys.* **1997,** *107*, 3032-3041.
86. Cossi, M.; Barone, V.; Cammi, R.; Tomasi, J., Ab Initio Study of Solvated Molecules: a New Implementation of the Polarizable Continuum Model. *Chem. Phys. Lett.* **1996,** *255*, 327-335.
87. Barone, V.; Cossi, M.; Tomasi, J., Geometry Optimization of Molecular Structures in Solution by the Polarizable Continuum Model. *J. Comput. Chem.* **1998,** *19*, 404-417.
88. Frisch, M. J.; Trucks, G. W.; Schlegel, H. B.; Scuseria, G. E.; Robb, M. A.; Cheeseman, J. R.; Scalmani, G.; Barone, V.; Petersson, G. A.; Nakatsuji, H.; Li, X.; Caricato, M.; Marenich, A. V.; Bloino, J.; Janesko, B. G.; Gomperts, R.; Mennucci, B.; Hratchian, H. P.; Ortiz, J. V.; Izmaylov, A. F.; Sonnenberg, J. L.; Williams-Young, D.; Ding, F.; Lipparini, F.; Egidi, F.; Goings, J.; Peng, B.; Petrone, A.; Henderson, T.; Ranasinghe, D.; Zakrzewski, V. G.; Gao, J.; Rega, N.; Zheng, G.; Liang, W.; Hada, M.; Ehara, M.; Toyota, K.; Fukuda, R.; Hasegawa, J.; Ishida, M.; Nakajima, T.; Honda, Y.; O. Kitao, O.; Nakai, H.; Vreven, T.; Throssell, K.; Montgomery Jr., J. A.; Peralta, J. E.; Ogliaro, F.; Bearpark, M.; Heyd, J. J.; Brothers, E.; Kudin, K. N.; Staroverov, V. N.; Keith, T.; Kobayashi, R.; Normand, J.; Raghavachari, K.; Rendell, A.; Burant, J. C.; Iyengar, S. S.; Tomasi, J.; Cossi, M.; Millam, J. M.; Klene, M.; Adamo, C.; Cammi, R.; Ochterski, J. W.; Martin, R. L.; Morokuma, K.; Farkas, O.; Foresman, J. B.; Fox, D. J., *Gaussian 09*. Gaussian Inc.: Wallingford, 2009.

For Table of Contents Only: